



 Cite this: *RSC Adv.*, 2021, **11**, 25122

# Photodegradation of pesticides using compound-specific isotope analysis (CSIA): a review†

 Guolu Cui,<sup>ab</sup> George Lartey-Young,<sup>ab</sup> Chong Chen<sup>ab</sup> and Limin Ma <sup>\*ab</sup>

Pesticides are commonly applied in agriculture to protect crops from pests, weeds, and harmful pathogens. However, chronic, low-level exposure to pesticides can be toxic to humans. Photochemical degradation of pesticides in water, soil, and other environmental media can alter their environmental fate and toxicity. Compound-specific isotope analysis (CSIA) is an advanced diagnostic tool to quantify the degradation of organic pollutants and provide insight into reaction mechanisms without the need to identify transformation products. CSIA allows for the direct quantification of organic degradation, including pesticides. This review summarizes the recent developments observed in photodegradation studies on different categories of pesticides using CSIA technology. Only seven pesticides have been studied using photodegradation, and these studies have mostly occurred in the last five years. Knowledge gaps in the current literature, as well as potential approaches for CSIA technology for pesticide monitoring, are discussed in this review. Furthermore, the CSIA analytical method is challenged by chemical element types, the accuracy of instrument analysis, reaction conditions, and the stability of degradation products. Finally, future research applications and the operability of this method are also discussed.

Received 2nd March 2021

Accepted 14th July 2021

DOI: 10.1039/d1ra01658j

[rsc.li/rsc-advances](http://rsc.li/rsc-advances)

## Introduction

Pesticides are chemicals that control and prevent arthropod pests, weeds, insects, and fungi in agriculture and urban environments.<sup>1</sup> The worldwide use of pesticides has significantly

increased since the 1960s. Pesticides can be categorized by chemical type, physical state, and main use (ESI,† Table) (the WHO Recommended Classification of Pesticides by Hazard and Guidelines to Classification 2009).<sup>2</sup> The listed chemical categories are included for convenience, and some pesticides may fall into more than one category.<sup>3</sup>

Pesticide production and use have increased globally with increased agricultural activity.<sup>4</sup> While pesticide application has addressed some of the problems associated with limited cropland and the food requirements of a growing global population,<sup>5</sup> after application, pesticide residue and runoff can lead to numerous environmental risks. Pesticide persistence,

<sup>a</sup>School of Environmental Science and Engineering, Tongji University, 1239 Siping Road, Shanghai 200092, China. E-mail: [lmma@tongji.edu.cn](mailto:lmma@tongji.edu.cn)

<sup>b</sup>Shanghai Institute of Pollution Control and Ecological Security, Shanghai 200092, China

† Electronic supplementary information (ESI) available. See DOI: 10.1039/d1ra01658j



*Ms Guolu Cui is a graduate student in the School of Environmental Science and Engineering, Tongji University. During her postgraduate studies, her main research interests are photodegradation of organic pesticides in water bodies and characterization of stable isotope fractionation.*



*George Lartey-Young is currently a PhD student under the guidance of Prof. Limin Ma at Tongji University, Shanghai, China P. R. His professional and research interests are in the areas of application of environmental monitoring tools and engineered carbon materials for remediation of water and soil contaminated media. Previously, he worked with Knight Pièsold Consulting, undertaking environmental monitoring and management programs for closure and reclamation of mine facilities.*



intrinsic toxicity, and their accumulation threaten the health of humans and the environment, and carcinogenesis and neurotoxicity are some of the potential adverse health effects that can result from pesticide exposure.<sup>6–8</sup> The degradation of pesticides in the natural environment mainly includes chemical, biodegradation,<sup>9</sup> and photodegradation.<sup>10</sup> Among these methods, photochemical degradation is dominant due to the abundance of solar light and its ability to destroy pesticides in surface soil and water, as well as plant surfaces and other media.<sup>11</sup> The photochemical reactions of pesticides in environmental matrices occur through direct and indirect photolysis.<sup>12</sup> During direct photolysis, the pesticide molecules become excited after absorbing UV or visible light energy and are transformed. The reaction pathways of indirect or sensitized photolysis include energy transfer, electron and hydrogen transfer, and the formation of reactive species, which involve the reactions of ground-state pesticides with other photochemically produced species in an environmental matrix.

Predicting the migration and transformation of pesticides in the environment requires a study on photodegradation mechanisms. Using current methods, mechanistic studies conducted in laboratory settings differ from degradation in the natural environment due to the lower concentrations in natural samples and interference from other compounds. However, compound-specific isotope analysis (CSIA) has a unique potential to bridge the differences of mechanism studies in the laboratory and natural environment.<sup>13</sup> CSIA offers a complementary approach for identifying contaminant sources and degradation pathways, as well as tracing the transformation reaction, even if several processes occur simultaneously. This can be accomplished by analysing the isotope ratios of single compounds and detecting and quantifying isotope fractionation.<sup>14</sup> CSIA also correlates well with existing methods to reveal pesticide degradation reactions, and can be used to quantify degradation and understand contaminant reaction mechanisms without the need for identifying transformation products.<sup>15</sup> The relative abundance ratios of isotopes can be described by calculating the stable isotope enrichment factors and further linking isotopic changes due to degradation to the extent of degradation using the Rayleigh fractionation model

(ESI<sup>†</sup>). The apparent kinetic isotope effect (AKIE) can also be used to compare the kinetic isotope effect of bond cleavage reactions of different molecules, while the isotope fractionation of two (or more) elements can be used to evaluate degradation pathways.<sup>16</sup> Thus, CSIA technologies have been used to study organic matter isotopic fractionation patterns for biodegradation, chemical substitution, and oxidation–reduction reactions of contaminants.<sup>17</sup>

However, there are still many gaps in CSIA technology that need to be addressed. First, elements that can use CSIA technology to determine stable isotope ratios remain limited.<sup>18</sup> Second, for pollutants such as pesticides, using CSIA is challenging, as it requires lower concentrations and pre-concentration information, purification, and high chromatographic performance.<sup>19</sup> In addition, isotope fractionation should be avoided during sample preparation to ensure the accuracy of the test results.<sup>20</sup> Thus, it is worth exploring how indirect photodegradation produces free radicals, as singlet-state oxygen does not occur during direct photolysis, and how using CSIA can be used to calculate the contributions of indirect photolysis and direct photolysis to degradation. Third, isotope fractionation originates not only from bond cleavages but also from the photophysical processes of excited states in photolytic transformations.

Therefore, it is important to study whether the photodegradation process of pesticides is accompanied by isotope fractionation and whether different pesticide types have unique isotope fractionation modes under the photodegradation pathway.<sup>17</sup> Light isotopic fractionation during degradation may result from the breaking of chemical bonds and may be due to the excited states of photophysical processes.<sup>21</sup> In this review, we summarize the photodegradation process and discuss its mechanisms and applications by using compound-specific isotope fractionation technologies on different types of pesticides. Furthermore, the utilization and analysis of the current status of photodegradation processes using CSIA technology are discussed, specifically in comparison to the study of biodegradation or hydrolysis by CSIA technology. We also forecast the future trends of CSIA applications for pesticide photodegradation.



*Dr Chong Chen has obtained a PhD in environmental science and engineering, and he has been working in the field of environmental behavior and risk assessment of persistent organic pollutants for the past few years. Presently he is working as a post-doctoral researcher at Tongji University.*



*Prof. Limin Ma has been working as a Professor in the School of Environmental Science and Engineering, Tongji University for many years. He is mainly engaged in research in the fields of ecological remediation of polluted environments, biogeochemistry, ecology, and past environmental changes. Recent topics of interest include application of compound stable isotope analysis (CSIA) tracer*

*principles and techniques.*



## Pesticide categories and CSIA technology

The current literature comprises of few studies on monitoring the photodegradation of pesticides using CSIA technology, and most of these studies were conducted in the last ten years (Table 1). The different studies for each category of pesticides are explained in detail in the following subsections.

### Organophosphorus compounds

Wu *et al.*<sup>22</sup> reported that OP esters are susceptible to hydrolysis, but photolytic degradation of dimethoate, a commonly known OP, was also used to demonstrate the utility of the CSIA method for different degradation mechanisms. The amide-acidic group in dimethoate was found to enhance the positive electrical properties of the phosphorus atom and therefore it hydrolysed rapidly in alkaline solutions. However, it was more stable in acidic solutions. In a comparative study of the acid hydrolysis of dimethoate using CSIA, only a slight enrichment of <sup>13</sup>C occurred. Under alkaline conditions, water molecules or OH<sup>-</sup> as nucleophilic reagents were found to be capable of bimolecular nucleophilic substitution reactions (S<sub>N</sub>2). Thus, a clear carbon isotope fractionation was observed during hydrolysis ( $\Delta\delta^{13}\text{C} = 1.9\%$ ). The carbon isotope enrichment factor ( $-1.0 \pm 0.1\%$ ) was significantly larger than the carbon isotope enrichment factor in the alkaline hydrolysis process of the organophosphorus pesticide dichlorvos ( $\epsilon_{\text{C}} = -0.2 \pm 0.1\%$ ), especially when combined with the hydrolysis paths of the two pesticides.<sup>23–25</sup> When combined with hydrolysis reaction mechanism studies, it can be hypothesized that under alkaline conditions, nucleophilic OH<sup>-</sup> attack on phosphorus atoms will lead to P–S bond cleavage without primary carbon isotope effects. Furthermore, the hydrogen atoms next to bond cleavage sites may produce secondary isotope effects. However, under neutral and acidic conditions, parallel nucleophilic OH attacks on C–O bonds may lead to C–O bond cleavage, and they are associated with primary stable carbon isotope effects. Thus, the two C–O bonds in dimethoate may break during photodegradation under direct UV irradiation.<sup>26</sup> In comparison, the photolysis of dimethoate caused a larger enrichment than hydrolysis. The carbon isotope fractionation factor was  $3.7 \pm 1.1\%$ , which was quantified by the Rayleigh model, providing a distinction between hydrolysis and photolysis. To further elucidate the reaction mechanism, AKIE values were calculated to characterize the isotopic effect of chemical bond breakage at the reaction site. Because it was unclear whether the photodegradation of dimethoate was a synergistic or stepwise reaction, only the AKIE values Table 1 were calculated and compared for both cases (Table 1) with a theoretical value of C–O bond breakage (1.061). Consequently, both values were found to be low. The kinetic isotope effect alone could not be used to determine the type of reaction during the photodegradation process of dimethoate. Thus, a weak depletion of carbon isotopes occurred during the initial stage of the reaction from zero to 5 h, though the reasons for this change were not discussed in the study.

Based on a direct photodegradation study of dimethoate, a more accurate prediction of the degradation mechanisms cannot be made using carbon isotopes alone. However, multi-element isotope analysis may be used to obtain information about OP pesticides through multi-element isotope analysis in future studies. Wu *et al.*<sup>27</sup> also highlighted the carbon and hydrogen fractionation patterns, which have the potential to reveal the transformation of ethyl parathion (EP) during direct photolysis and OH radical oxidation induced by UV/H<sub>2</sub>O<sub>2</sub> photolysis. In this case,  $\epsilon_{\text{C}}$  was low compared with dimethoate, and no detectable  $\epsilon_{\text{H}}$  was observed during both experiments of EP. Therefore, combining the photodegradation products of EP with the analysis of the direct photolysis conversion mechanisms and OH radical oxidation processes, suggested that the rate-limiting step of EP was proceeded by an oxidative attack on the P=S bond by an OH radical to the central phosphorus atom, yielding a phosphorenyl radical. This was stationed by the elimination of a sulfhydryl radical to produce P=O, or the elimination of nitrophenol from the phosphoric center. None of the presumed direct C single bond breakage mechanisms were involved, which verified that the primary isotope effect did not occur with the low values of the carbon isotope enrichment factor. This meant that the carbon and nitrogen isotope enrichment factor could not be used to distinguish direct photodegradation from indirect photolysis. Photosensitizers that promote indirect photolysis are also naturally occurring degradation processes that are important for the production of free radicals, such as hydroxyl radicals, which are required for photodegradation and are important for controlling the fate of organic pollutants in the environment.<sup>44</sup> In conclusion, multiple isotope fractionation patterns characterize the bond cleavage mechanisms of photosensitization and are therefore valuable tools for studying the fate of pesticides in surface water and atmospheric media containing photosensitizers. Likewise, the pH value causes changes in the reaction mechanism of the degradation process, and carbon and hydrogen isotope enrichment factors have been measured for the hydrolysis of dimethoate under different pH conditions. The values of  $\epsilon_{\text{C}}$  were smaller and  $\epsilon_{\text{H}}$  larger under alkaline conditions, whereas the opposite was true for neutral conditions (Table 1). In combination with the hydrolysis reaction mechanism study,<sup>45</sup> it is possible that under alkaline conditions, the attack of nucleophilic OH<sup>-</sup> on the phosphorus atom will lead to P–S bond cleavage without the primary carbon isotope effect, and the hydrogen atom next to the bond cleavage site may produce a secondary isotope effect. However, under neutral and acidic conditions, the attack of parallel nucleophilic OH<sup>-</sup> on the C–O bond may lead to C–O bond cleavage, and is associated with the primary stable carbon isotope effect. Furthermore, tributyl phosphate (TBP) is an OP compound used in herbicide formulations. Liu *et al.*<sup>46</sup> used TBP as a model compound to study stable isotope fractionation associated with bond cleavage reactions. The results showed that identifying radical reactions and distinguishing hydrolysis processes was determined by correlating the <sup>2</sup>H and <sup>13</sup>C isotope fractionation of TBP. This revealed that dual isotope analysis has diagnostic value. The photodegradation process is also influenced by pH. Thus, it



Table 1 Photodegradation studies of pesticides conducted with compound-specific isotope analysis<sup>a</sup>

Pesticide	Structural formula	Category	Degradation type	$\epsilon_{\text{element}} (\text{‰})$	AKIE <sub>element</sub>	Reference
Dimethoate		OP	Direct photolysis	$\epsilon_{\text{carbon}} = (-3.7 \pm 1.1)\text{‰}$	AKIE <sub>C</sub> = 1.0094 ± 0.0027 or 1.0188 ± 0.0054	Wu <i>et al.</i> <sup>22</sup>
			Alkaline hydrolysis	$\epsilon_{\text{carbon}} = (-1.0 \pm 0.1)\text{‰}$	AKIE <sub>C</sub> = 1.0050 ± 0.0005	Wu <i>et al.</i> <sup>22,28</sup>
			Neutral hydrolysis	$\epsilon_{\text{hydrogen}} = -10\text{‰}$	n.d.	
				$\epsilon_{\text{carbon}} = (-8.3 \pm 0.3)\text{‰}$		
				$\epsilon_{\text{hydrogen}} = 0 + 1\text{‰}$		
				$\Delta\delta^{13}\text{C} = 0.2\text{‰}$		
Parathion		OP	Acidic hydrolysis	$\epsilon_{\text{carbon}} = (-0.6 \pm 0.1)\text{‰}$	n.d.	
			Direct photolysis	$\epsilon_{\text{hydrogen}} \approx 0\text{‰}$	n.d.	
			Indirect photolysis	$\epsilon_{\text{carbon}} = (-0.8 \pm 0.1)\text{‰}$	n.d.	Wu <i>et al.</i> <sup>27</sup>
				$\epsilon_{\text{hydrogen}} \approx 0\text{‰}$		
			Alkaline hydrolysis	$\epsilon_{\text{carbon}} = (-6.0 \text{ to } -3.5)\text{‰}$	n.d.	
			Acidic hydrolysis	$\epsilon_{\text{carbon}} = (-6.9 \text{ to } -6.7)\text{‰}$	n.d.	
Glyphosate		OP	Direct photolysis	$\delta^{18}\text{O}$	n.d.	Sandy <i>et al.</i> <sup>29</sup>
Chloroaniline		Other	2-Cl-aniline:	$\epsilon_{\text{carbon}} = (+1.5 \pm 0.5)\text{‰}$	AKIE <sub>C</sub> = 0.9909 ± 0.0014	
				$\epsilon_{\text{nitrogen}} = (-2.9 \pm 0.3)\text{‰}$	AKIE <sub>N</sub> = 1.0029 ± 0.0002	
			3-Cl-aniline:	$\epsilon_{\text{carbon}} = (-0.4 \pm 0.1)\text{‰}$	AKIE <sub>C</sub> = 1.0024 ± 0.0006	
				$\epsilon_{\text{nitrogen}} = (-1.7 \pm 0.2)\text{‰}$	AKIE <sub>N</sub> = 1.0017 ± 0.0002	Ratti <i>et al.</i> <sup>30,31</sup>
			4-Cl-aniline:	$\epsilon_{\text{carbon}} = (-1.2 \pm 0.2)\text{‰}$	AKIE <sub>C</sub> = 1.0073 ± 0.0012	
				$\epsilon_{\text{carbon, CsCl}} = (-1.8 \pm 0.3)\text{‰}$	AKIE <sub>N</sub> = 1.0012 ± 0.0002	
HCH		OC	Direct photolysis	$\epsilon_{\text{carbon, CsCl}} = (-2.3 \pm 0.3)\text{‰}$	AKIE <sub>C</sub> = 1.017 ± 0.001	Zhang <i>et al.</i> <sup>32</sup>
			Indirect photolysis	$\epsilon_{\text{carbon}} = (-2.8 \pm 0.2)\text{‰}$	AKIE <sub>C</sub> = 1.012 ± 0.001	
			Alkaline hydrolysis	$\epsilon_{\text{carbon}} = (-1.9 \pm 0.2)\text{‰}$	AKIE <sub>C</sub> = 1.048 ± 0.003	Badea <i>et al.</i> , <sup>33</sup> Zhang <i>et al.</i> <sup>32</sup>
			Biodegradation	$\epsilon_{\text{carbon}} = (-7.6 \pm 0.4)\text{‰}$	AKIE <sub>C</sub> = 1.015 to 1.023	
				$\epsilon_{\text{carbon}} = (-3.7 \text{ to } -1.0)\text{‰}$		
				$\epsilon_{\text{carbon}} = (4.6 \pm 0.3)\text{‰}$		
Atrazine		T	Direct photolysis	$\epsilon_{\text{nitrogen}} = (4.9 \pm 0.2)\text{‰}$	n.d.	Hartenbach <i>et al.</i> <sup>34</sup>
			Indirect photolysis	$\epsilon_{\text{hydrogen}} \approx 0\text{‰}$	AKIE <sub>H</sub> = 1.3 to 2.7	Khan <i>et al.</i> , <sup>35</sup> Meyer <sup>36</sup>
				$\epsilon_{\text{carbon}} = (-0.5 \text{ to } -1.7)\text{‰}$		
				$\epsilon_{\text{nitrogen}} = (-0.3 \text{ to } -0.7)\text{‰}$		
				$\epsilon_{\text{hydrogen}} \approx (-2.5 \text{ to } -51)\text{‰}$		
				$\epsilon_{\text{carbon}} = (-5.6\text{‰} \pm 0.1)\text{‰}$	AKIE <sub>C</sub> = 1.047 ± 0.006	Meyer <i>et al.</i> <sup>37</sup>
Isoproturon		Other	Alkaline hydrolysis	$\epsilon_{\text{carbon}} = (-1.2\text{‰} \pm 0.1)\text{‰}$	AKIE <sub>C</sub> = 1.001 ± 0.001	Masbouh <i>et al.</i> <sup>38</sup>
			Acidic hydrolysis	$\epsilon_{\text{carbon}} = (-6.1\text{‰} \pm 0.8)\text{‰}$	AKIE <sub>C</sub> = 1.052 ± 0.006	
			Biodegradation	$\epsilon_{\text{nitrogen}} = (1.3\text{‰} \pm 0.6)\text{‰}$	AKIE <sub>N</sub> = 0.994 ± 0.001	Chen <i>et al.</i> <sup>39</sup>
				$\epsilon_{\text{carbon}} = (-1.4 \text{ to } -5.4)\text{‰}$	AKIE <sub>C</sub> = 1.011 to 1.045	
				$\epsilon_{\text{nitrogen}} = (0.8 \text{ to } 3.3)\text{‰}$	AKIE <sub>N</sub> = 0.974 to 0.996	Yu <i>et al.</i> <sup>40</sup>
				$\epsilon_{\text{carbon}} = (-0.018 \pm 0.006)\text{‰}$	n.d.	





Table 1 (Contd.)

Pesticide	Structural formula	Category	Degradation type	$\epsilon_{\text{element}} (\text{‰})$	AKIE <sub>element</sub>	Reference
Bromoxynil		Other	Indirect photolysis	$\delta^{15}\text{N} = (-15.148 \pm 0.76)\text{‰}$ $\epsilon_{\text{carbon}} = (-0.002 \pm 0.001)\text{‰}$ $\delta^{15}\text{N} = (-14 \text{ to } -16)\text{‰}$	n.d.	Penning and Elsner <sup>41</sup> Penning <i>et al.</i> <sup>42</sup>
		Other	Hydrolysis Biodegradation	$\epsilon_{\text{carbon}} = (-5.7 \pm 0.2)\text{‰}$ $\epsilon_{\text{carbon}} = (-5.7 \pm 0.2)\text{‰}$ $\epsilon_{\text{nitrogen}} = (-3.3 \pm 0.4)\text{‰}$ $\epsilon_{\text{carbon}} = (0.34 \pm 0.44)\text{‰}$ $\epsilon_{\text{nitrogen}} = (-3.7 \pm 0.3)\text{‰}$ $\epsilon_{\text{carbon}} = (4.74 \pm 0.82)\text{‰}$ $\epsilon_{\text{nitrogen}} = (0.76 \pm 0.12)\text{‰}$	n.d. n.d.	

" n.d. denotes "not discussed" .

is worthwhile to investigate whether fractionation of different carbon, hydrogen, or other isotopes also occurs.

Organophosphorus pesticides include a variety of phosphorothioate (*e.g.*, EP) and dithiophosphorothioate (*e.g.*, dimethoate) salts, while some organophosphorus pesticides are phosphates. Also, tris(2-carboxyethyl)phosphine (TCEP), which is a synthetic phosphate substance, was observed by carbon and hydrogen isotope fractionation during the indirect photo-degradation process ( $\epsilon_{\text{C, UV/H}_2\text{O}_2} = -1.4 \pm 0.1\text{‰}$ ;  $\epsilon_{\text{H, UV/H}_2\text{O}_2} = -56 \pm 3\text{‰}$ ), and it was postulated that hydroxyl radicals could undergo C–H bond cleavage during photooxidation, resulting in H abstraction.<sup>27</sup> The P–O bonds in phosphates are resistant to inorganic hydrolysis, thus any changes observed in oxygen isotope composition ( $^{18}\text{O}/^{16}\text{O}$ ) may be used as a signature to distinguish phosphonates from phosphor-esters and organophosphorus, due to the changes in the phosphate  $\delta^{18}\text{O}$ .<sup>47,48</sup> Sandy *et al.*<sup>29</sup> used the oxygen isotope labelling of ambient water and atmospheric oxygen, and hypothesized that photoexcited water produces hydroxyl radicals, while atmospheric oxygen produces peroxy radicals for nucleophilic substitution reactions. Consequently, the C–P bonds break based on changes in  $\delta^{18}\text{O}$  in the reactants and degradation products, combined with the models and reaction mechanisms. Humic acids have also been found to absorb UV light and act as photosensitizers, and can promote the photo-oxidation of bound glyphosate, which is a phosphate herbicide, forming reactive intermediates such as singlet oxygen. Zakon *et al.*<sup>49</sup> studied both carbon and bromine isotope effects during UV-photolysis of bromophenols and found a correlation between isotope fractionation and the potential reaction mechanism of profenofos. The anomalous inverse bromine isotope (up to +5.1‰) and carbon isotope effects (from –12.6‰ to –23.4‰) were associated with molecule photoexcitation. This interesting inversion as a result of Br fractionation was due to the magnetic field isotope effect (mass-independent isotope effect, MIE) during the photochemical reaction.<sup>50,51</sup> MIE is a mass-independent isotopic effect caused by the magnetic field interactions between the electron and the spin-generating nucleus, resulting in the generation of free radical pairs with different spin states. Chemical reactions are spin-selective, so significant MIE occurs for nuclei composed of zero-spin and non-zero-spin isotopes (ESI†). The element bromine has two stable isotopes, <sup>79</sup>Br (2.7089) and <sup>81</sup>Br (2.9210), which, although they have the same nuclear spin, have different magnetic points and therefore impose different ultrafine interactions on the electron spins. This in turn affects the spin conversion rate and leads to the observed Br isotope effect. This conjecture has also been mentioned in the photodegradation reaction of triazine pesticides.

Tang *et al.*<sup>52</sup> assessed the extent and mechanisms involved in the biodegradation of chlorpyrifos using CSIA for different types of integrated recirculating constructed wetlands. Similar studies were also performed<sup>53,54</sup> on six pyrethroids (bifenthrin, fenpropathrin, permethrin,  $\alpha$ -cypermethrin, fenvalerate, and deltamethrin), using CSIA to estimate their bioavailability (ESI†). The photodegradation of OP diazinon was a potential source of eutrophication in water, including direct and indirect photolysis, because phosphate was released following diazinon

photodegradation.<sup>55</sup> High-performance liquid chromatography coupled with electrospray ionization quadrupole time-of-flight mass spectrometry (HPLC-ESI-Q/TOF-MS) analysis indicated that the photodegradation of diazinon was initiated by cleavage of the P–O bond.<sup>56</sup> Compound oxygen stable isotope analysis was used to verify the release pathway of phosphates from diazinon degradation in the Fe(III)–oxalate complex system. In addition, CSIA was applied to distinguish commercial glyphosate produced by different brands or manufacturers based on  $\delta^{15}\text{N}$  and  $\delta^{13}\text{C}$ , and trace the source of glyphosate and AMPA according to the magnitude of the value. Kujawinski *et al.*<sup>57</sup> suggested that carbon isotope ratio ( $^{13}\text{C}/^{12}\text{C}$ ) measurements allow for the study of the glyphosate chemical source or sources. Mogusu *et al.*<sup>58</sup> provided a compound-specific  $^{15}\text{N}/^{14}\text{N}$  analysis of glyphosate and aminomethylphosphonic acid (AMPA) in a two-step derivatization process during oxidative degradation. This process focused on abiotic degradation, and the research complemented the results of Kujawinski *et al.*<sup>57</sup> A double isotope also better detects the aminoacylation of glyphosate and AMPA molecules. The results thus confirmed that different pH values influence the derivatization of the N–H group during the isopropyl chloroformate processes. Of these, buffering solutions at pH 10 were critical for obtaining accurate nitrogen isotope ratios. In conclusion, the main difference between phosphorothioate and dithiophosphorothioate is the sulfur content. Because oxygen is more electronegative than sulfur and has a greater electron-absorbing capacity, we speculate that the enhanced positivity of the phosphorus atom is greater, allowing the P=S in phosphorothioate (*e.g.*, EP) to oxidize to P=O in a rate-determining step, resulting in minimal or no carbon and hydrogen fractionation. Conversely, the dithiophosphorothioate (*e.g.*, dimethoate) undergoes C-containing side-chain breakage, resulting in higher carbon fractionation. For phosphate structures replaced by alkyl groups (*e.g.*, glyphosate), the mechanism of C–P bond breakage needs to be further analysed and verified using carbon isotopes.

### Organochlorine compounds

Hexachlorocyclohexanes (HCHs) have been used as insecticides since 1942, and are of great environmental concern because of their bioaccumulation and persistence.<sup>59</sup> Zhang *et al.*<sup>32</sup> compared the direct photolysis and indirect photolysis (UV/ $\text{H}_2\text{O}_2$ ) of  $\alpha$ -HCH with biodegradation and quantified carbon isotope enrichment factors ( $\epsilon_{\text{C}}$ ). Hydrogen abstraction by hydroxyl radicals due to UV/ $\text{H}_2\text{O}_2$  led to an  $\epsilon_{\text{C}}$  of  $-1.9 \pm 0.2\%$  with an apparent kinetic carbon isotope effect (AKIE<sub>C</sub>) of  $1.012 \pm 0.001$ . The obtained carbon isotope fractionation value was smaller than the value during direct photodegradation ( $\epsilon_{\text{C}} = -1.9 \pm 0.2\%$ ), which may have been due to the different types of rate-limiting reactions. While the direct photodegradation process considers the rate-limiting step to be dechlorination through cleavage of single-bonded C–Cl, which occurs directly with breakage of single-bonded carbon, a moderate degree of carbon isotopic fractionation was observed ( $\epsilon_{\text{C}} = -2.8 \pm 0.2\%$ ). This phenomenon was consistent with the change in  $\epsilon_{\text{C}}$  when H abstraction occurred at TCEP, as described above ( $\epsilon_{\text{C}} = -1.4 \pm$

$0.1\%$ ). It is also possible to estimate a numerical range of carbon isotope enrichment factors for the H abstraction process. The initial step of hydrolysis should be the simultaneous cleavage of the C–H and C–Cl bonds through a bimolecular synergistic elimination reaction, thus resulting in a larger and maximum carbon isotope fractionation ( $\epsilon_{\text{C}}$  of  $-7.6 \pm 0.4\%$ ) compared to the photolysis process, which cleaves only the C–Cl and H-abstracted carbon isotopes. The binding of the substrates to enzymes during biodegradation reduces the degree of carbon isotope fractionation, and thus the degree of fractionation will be lower compared to hydrolysis.<sup>60</sup> Thus, we were able to validate and complement the apparent kinetic effects (AKIE<sub>C</sub> values) of different types of carbon isotopes for different processes, such as OH radical-induced H extraction, C–H bond breaking, dehydrogenation, and homogeneous cleavage of C–Cl bonds. Ivdra *et al.*<sup>61,62</sup> used carbon, hydrogen, and chlorine stable isotope fingerprinting, specifically the most positive  $\delta^2\text{H}$ ,  $\delta^{13}\text{C}$ , and  $\delta^{37}\text{Cl}$  values, as baselines and considered  $^2\text{H}$ ,  $^{13}\text{C}$ , and  $^{37}\text{Cl}$ -enriched HCHs as evidence of the degradation processes. In other studies, Badea *et al.*<sup>33</sup> used a gas chromatography-combustion-isotope ratio mass spectrometry (GC-C-IRMS) system equipped with carbon isotopes to reveal  $\delta$ -values of  $-32.5 \pm 0.8\%$  and  $-32.3 \pm 0.5\%$  for (–)–HCH and (+)–HCH, respectively. HCHs and major stereoisomers ( $\alpha$ -,  $\beta$ -,  $\delta$ - and  $\gamma$ -HCHs) were degraded most efficiently on a  $2.24 \text{ mg cm}^{-2}$   $\text{TiO}_2$  thin film under 400 W of UV irradiation at 365 nm and a high-pressure mercury lamp.<sup>63,64</sup> This meant that CSIA can be used to identify the manufacturer and source of the HCHs, as well as assess the different degradation types of  $\alpha$ -HCHs.

Due to the large  $\Pi$  bond on the benzene ring and the low polarity of chlorobenzenes, chlorinated organochlorine pesticides are structurally stable, and the benzene ring is not easily broken. Therefore, compound-specific isotope analysis of chlorine (CSIA- $\delta^{37}\text{Cl}$ ) is commonly used to provide quantitative data on the transport and transformation of chlorinated organochlorine pesticides. Dichloro diphenyltrichloroethane (DDT) is an organochlorine pesticide that was banned in 1983 in many countries, including China. Most DDT studies involve source analysis and use CSIA as an indicator,<sup>65</sup> while some studies have focused on the biodegradation process<sup>66</sup> analysis for DDT. The main degradation products of DDT are 1,1-bis-(4-chlorophenyl)-2,2-dichloroethene (DDE) and 1-chloro-4-[2,2-dichloro-1-(4-chlorophenyl)ethyl]benzene (DDD). CSIA-Cl has been used to study the degree of degradation of bioaccumulating persistent organic pollutants (POPs) at environmental concentrations. The apparent enrichment of  $^{37}\text{Cl}$  in DDT and 1,1-(dichloroethenylidene)bis(chloro-benzene) (DDE) derives from the kinetic isotope effect (KIE) associated with the environmental degradation of DDT, but has not been shown to involve biological or abiotic factors ( $\delta^{37}\text{Cl}$ , DDT =  $-0.69 \pm 0.21\%$ ,  $\delta^{37}\text{Cl}$ , DDE =  $-2.98 \pm 0.57\%$ ).<sup>67</sup> However, issues related to the differences in chlorine isotope fractionation between DDT and its derivatives by compound-specific chlorine/bromine isotope analysis (CSIA-Cl/Br) have received considerable attention. Cl/Br isotope fractionation of DDT has been studied by gas chromatography-mass spectrometry (GC-MS) or GC double-focusing magnetic sector high-resolution mass spectrometry (GC-DFS-HRMS).<sup>68,69</sup> GC-DFS-



HRMS, with its unique dual-GC formulation and mass calibration that is independent of scan speed, polarity, and ionization mode, exhibits exceptional specificity and sensitivity compared to other GC-MSs. However, CSIA results are equally affected by peak retention time and peak shape. The results have shown that *o,p'*-DDT (37.4‰) and *p,p'*-DDT (36.0‰) are similar in terms of chlorine isotope fractionation, with brominated compounds showing opposite isotope fractions and lower isotope fractions than chlorinated compounds.

CSIA studies related to hexachlorobenzene (HCB) have focused on experimental methods such as the fractionation of chlorine and bromine isotopes on gas chromatographic columns,<sup>68</sup> and the fractionation of chlorine and bromine isotopes during fragmentation by gas chromatography-electron ionization high-resolution mass spectrometry.<sup>69</sup> However, they did not focus on photodegradation. Rather, HCB was used as a typical chlorinated aromatic compound and the effect of the solvent on its photodegradation pathway and products was evaluated. The photodechlorination of HCB and other chlorinated benzenes (CBz) have also been analysed.<sup>70</sup> Understanding this trend and analyzing degradation mechanisms using new technologies such as CSIA will therefore allow us to predict the molecular structures of the main products.<sup>70</sup> Isotope-related analytical methods have been evaluated, and determining the chlorine isotope abundance ratios of HCB using gas chromatography-high resolution time-of-flight mass spectrometry (GC-HR-TOF MS) has been studied.<sup>71</sup> This method is expected to be used for characterizing and studying the degradation process of organochlorine pollutants. The CSIA-Cl/Br method using GC-HR-TOF MS significantly simplifies sample pretreatment; however, asymmetric and/or broad peaks that appear during analysis make it difficult to accurately integrate peak areas, which affects the accuracy of the CSIA results. Consequently, GC-IRMS is limited to the analysis of certain compounds and molecular fragments by fixed Faraday detector alignments. CSIA has been used to evaluate the biodegradation of HCB and monitoring the *in situ* microbial reductive dehalogenation of highly halogenated benzene by carbon isotope fractionation.<sup>72</sup>

Triadimefon (TDF) [(*R,S*)-1-(4-chlorophenoxy)-3,3-dimethyl-1-(1*H*-1,2,4-triazol-1-yl)butan-2-one] is a chiral systemic broad-spectrum 1,2,4-triazole fungicide and organochlorine pesticide used for controlling plant diseases and insect pests. More than 30% of pesticides are chiral.<sup>73</sup> When triadimefon was added to 100% of D<sub>2</sub>O and H<sub>2</sub>O, the racemization rate revealed significant isotope effects, suggesting that the rate-determining step is the cleavage of the C–H (C–D) bond<sup>73</sup> during the racemization of triadimefon. Thus, methods that use isotopes in the detection of triadimefon and other pesticides involve establishing an isotope-labelled internal standard method of various pesticides or even mixtures.<sup>74</sup> The photophysics and photochemistry of triadimefon have also been associated with other factors, such as irradiation wavelength and solvent.<sup>75,76</sup> Studies related to CSIA of triadimefon have not been conducted. Specifically, chlorinated organochlorine pesticides, such as DDT, HCB, and chlorothalonil, characterize the photodegradation processes using CSIA-Cl because of their stable

benzene ring structure and the absence of alkyl- or nitrogen-containing side chains. However, the differences in molecular volume between the heavier and lighter chlorine isotopes, for example, the differences in vibrational frequency, bond energy, and length of the intramolecular bonds, are less pronounced.<sup>77</sup> Chlorine isotopic fractionation thus is more difficult to observe and requires a more precise method development, whereas chlorinated organochlorine pesticides such as TDF, which have carbon or nitrogen-containing side chains, can be degraded using multiple isotopes if photodegradation occurs with side chain breaks and if isotopic fractionation follows the kinetic isotope effect.

### Triazine derivatives

Atrazine (2-chloro-4-ethylamino-6-isopropylamino-*s*-triazine) is one of the most widely used herbicides and is of special interest<sup>35</sup> due to its ready transport in the environment.<sup>78</sup> Photodegradation of atrazine and other *s*-triazine herbicides have been studied,<sup>79</sup> and most studies focused on LC-MS/MS and GC-MS techniques. Researchers often use atrazine as a model substance for atrazine pesticides because both atrazine and atrazine share the same structural characteristics such as a triazine ring, and some of the side chains are identical. Furthermore, it has a relatively simple structure, a wide range of use, and a diversity of degradation products and mechanisms such as photolysis, hydrolysis, and biodegradation. Nearly 35 different atrazine degradation by-products have been characterized, including hydroxyatrazine, desethylatrazine, and desisopropylatrazine.<sup>35,80</sup> Dual element isotope fractionation ( $\delta^{13}\text{C}$  vs.  $\delta^{15}\text{N}$ ) showed characteristic carbon and nitrogen isotope patterns during the alkaline hydrolysis of atrazine,<sup>36</sup> and isotopic enrichment factors  $\epsilon_{\text{carbon}} = -5.6\text{‰} \pm 0.1\text{‰}$  and  $\epsilon_{\text{nitrogen}} = -1.2\text{‰} \pm 0.1\text{‰}$  were obtained. Based on the alkaline hydrolysis mechanisms of atrazine, and the differences between the carbon and nitrogen isotope enrichment factors, it is believed that carbon isotope fractionation is due to the primary isotopic effect produced by the nucleophilic aromatic substitution of heterocyclic atrazine due to the substitution of Cl by OH. Although nitrogen isotope fractionation occurs even though the nitrogen atoms are neither bonded nor unbonded during the reaction, and the nitrogen isotope enrichment factor is small but not negligible, the nitrogen isotope effect in this reaction is presumed to be secondary. This is because all of the nitrogen atoms are embedded in the aromatic  $\pi$ -system, which is disturbed by the C–Cl position reaction. The model-calculated values of the apparent kinetic effects also validate the mechanism of atrazine alkaline hydrolysis by demonstrating that the nitrogen atoms embedded in the aromatic  $\pi$  system are also involved in the nucleophilic substitution reaction. The primary carbon isotope effect of a given element present in a C–Cl bond of atrazine is position-specific. However, an opposite effect,  $\epsilon_{\text{N}} = 1.3 \pm 0.6\text{‰}$ , has been observed under acidic conditions, possibly due to the additional step of protonation at one of the N atoms.<sup>81</sup> Carbon isotopic fractionation does not significantly vary, which implies the same disruption of C–Cl single bond.



For the same reaction, each molecular position has a different isotope effect, and the same position shows different isotope effects in different reactions. One set of results reported by Hartenbach *et al.*<sup>34</sup> showed very different results for  $\epsilon_{\text{carbon}}$  and  $\epsilon_{\text{nitrogen}}$  during photolytic transformation (Table 1) compared to a parallel study on atrazine hydrolysis. The studies have associated  $^{13}\text{C}$ ,  $^2\text{H}$ , and  $^{15}\text{N}$  fractions with light-induced transformations of atrazine under neutral conditions. Furthermore, the  $^{13}\text{C}$  and  $^2\text{H}$  enrichment factors for use of 34-CBBP\* as an oxidant in the photo-oxidation process were about two to three times higher than those of  $\cdot\text{OH}$  as an atrazine oxidant. This may be due to the fractionation of C and H isotopes, which was mainly caused by the breakage of the N-isopropyl side chain and/or the N-ethyl side chain during atrazine photo-oxidation. However,  $^3\text{4-CBBP}^*$  as an oxidant, is more selective for the reaction of these two side chains, thus can change the values of the isotope enrichment factors. Nevertheless, despite the differences in values, both oxidants result in the enrichment of C and H isotopes, indicating linear enrichment relationships. The less pronounced difference in N isotope fractionation may be the result of the homotriazole benzene ring staying intact during the reaction, causing a secondary kinetic isotope effect in N isotope fractionation. This is consistent with the trend of N isotope fractionation during hydrolysis, and the numerical changes are not significant. On the contrary, an inverse isotope fractionation of  $^{13}\text{C}$  and  $^{15}\text{N}$  during the reaction of direct atrazine photolysis occurs, and the enrichment of  $^2\text{H}$  is almost identical to the control  $\delta^2\text{H}$  trend, suggesting that the changes in the atrazine  $\delta^2\text{H}$  may not be related to direct photolysis. This shows that the triazine ring is mainly involved in the photochemical transformation of the reaction mechanism. The first hypothesis is that atrazine in excited mono- and triplet states will return to lower energy levels by radiation-free jumps,<sup>82</sup> such as vibrational relaxation and internal transfer, and/or returns to the fundamental state by radiative jumps, such as fluorescence or phosphorescence, resulting in depletion of the  $^{13}\text{C}$  and  $^{15}\text{N}$  isotopes. However, this speculation cannot be currently quantified or measured, and therefore lacks sufficient evidence. The second hypothesis is that the nuclear spins of different isotopes differ in the number of spins in the nucleus (*i.e.*,  $^{13}\text{C}$  (spin 1/2) *vs.*  $^{12}\text{C}$  isotopologues (no spin) or  $^{15}\text{N}$  (spin 1) *vs.*  $^{14}\text{N}$  (spin 1/2)). Consequently, the nuclear spins act as “applied magnetic energies”, starting the non-equilibrium spin transition process of the excited state atrazine radical pairs, thus affecting the triazine ring. Thus, the magnetic interaction of the excited state species, specifically the magnetic isotope effect rather than the kinetic isotope effect, is the dominant factor. This magnetic field effect has been proposed by Buchachenko<sup>83</sup> for photochemical reactions involving species with unpaired electrons, but still needs to be supported by more relevant studies. The slope of direct photolysis was found to be  $1.05 \pm 0.14$  (two-dimensional isotope analysis of  $\Delta\delta^{15}\text{N}/\Delta\delta^{13}\text{C}$ ), which is significantly different from the slopes observed for photooxidation of atrazine with  $^3\text{4-CBBP}^*$  and OH radicals.<sup>34</sup> The study of photolysis of atrazine illustrates that CSIA can be used to distinguish between direct and indirect phototransformation pathways of pesticides in the environment.

During atrazine biodegradation, carbon isotope enrichment factors were negative among the different species of degrading bacteria, and nitrogen isotope enrichment factors were positive. However, the inverse nitrogen isotope effect was in agreement with the results obtained from abiotic hydrolysis ( $\epsilon_{\text{carbon}} = (-1.4 \text{ to } -5.4)\text{‰}$ ,  $\epsilon_{\text{nitrogen}} = (0.8 \text{ to } 3.3)\text{‰}$ ),<sup>39</sup> indicating triazine ring protonation.<sup>39</sup> However, this was different from the depletion that occurs during nitrogen isotope fractionation in indirect photolysis, where the kinetic isotope effect is still the dominant, secondary kinetic isotope effect. Thus, the values of the C and N enrichment factors differed, depending on the location and effect of the degrading bacteria. A comparison of hydrolysis, biodegradation, and photolysis studies of atrazine using CSIA indicated that CSIA can quantify the degree of bond breakage, and consequently degradation, for different reaction types. For example, no hydrogen isotope fractionation was observed during direct photodegradation, indicating that the triazine ring is the fraction involved in the photochemical transformation of atrazine. The large differences in the values of carbon and nitrogen isotopes also indicate a significant correlation between the primary and secondary isotopic effects and the degree of isotopic fractionation, while the occurrence of carbon and nitrogen isotopic anti-patterns during direct photodegradation confirm that isotopic effect type causing the fractionation, as well as the type of nucleophilic substitution reaction, can affect the results.

In the photolysis study of atrazine using CSIA, only photolysis under neutral conditions was studied. Nevertheless, it is still worth investigating whether the acid–base conditions will cause the same CSIA results, as well as analysing the degradation mechanism using this technique for the hydrolysis process. Recent studies<sup>84</sup> have pointed out that photosensitizers, as triplet dissolved organic matter, will also affect the photodegradation process of atrazine. How the fractionation of stable carbon and nitrogen isotopes and the size of the enrichment factor change during the photosensitization reaction should also be investigated. Thus, we infer that the photodegradation of ametryn and other atrazine substances, such as cyanazine, propazine, and simazine, can be productively studied using CSIA technology, and many other influencing factors should be considered.

### Pyrethroids

Analysis of pyrethroids and pyrethroids in combination with CSIA has not been frequently reported, and analytical methods have progressed from GC<sup>85</sup> toward LC-MS/MS or GC-MS/MS.<sup>86</sup> Ultra-performance liquid chromatography-tandem mass spectrometry (UPLC-MS-MS) has been used to identify and quantify residues and metabolites of 15 selected pyrethroids.<sup>87</sup> Furthermore, eight pyrethroid pesticide analogues can be quantified using negative chemical ionization gas chromatography with the assistance of mass spectrometric detection (NCI-GC-MS),<sup>88</sup> using a stable isotope as the internal standard. This includes deuterium labeling, for the correction of matrix effects and instrument variability. The photodegradation pathways of pyrethroids include four main groups: isomerization, 3,3-





dimethacrylate formation, ester bond cleavage and related pathways (C–C, O–C bond cleavage), as well as decarboxylation and reductive dehalogenation.<sup>89</sup> Therefore, if the photodegradation process of pyrethroids can be predicted by carbon stable isotope analysis, the enrichment of <sup>13</sup>C can be observed, and it is worthwhile to analyse whether the *cis-trans* isomerization affects the vibration strength of the bond and, thus, CSIA analysis.

Pyrethroid degradation studies with compound-specific stable isotope assays have focused on biodegradation, using CSIA to study the microbial degradation of lambda-cyhalothrin in soil.<sup>90</sup> Changes in the carbon isotope ratio have been observed, and the enrichment factor  $\epsilon$  of lambda-cyhalothrin has been identified. This may be because soil biodegradation is mainly responsible for lambda-cyhalothrin disintegration. Similarly, CSIA can be used for qualitative detection of biodegradation, and the quantitative assessment of biodegradation<sup>53</sup> rates during alpha-cypermethrin decay. The enrichment factor  $\epsilon$  was  $-1.87\%$ , and there was a positive correlation between the microbial degradation percentage and soil organic carbon content.<sup>91</sup> Thus, CSIA was developed to assess the bioavailability of six pyrethroids (bifenthrin, fenprothrin, permethrin,  $\alpha$ -cypermethrin, fenvalerate, and deltamethrin) under soil microbial degradation conditions using stable carbon isotope ratios, and to characterize trends in the bioavailability of pyrethroids and reduce abiotic elimination interference.<sup>54</sup>

Studies on CSIA for pyrethroids have also been explored in the context of chemical reactions. Dichlorobenzenes (DCBs) occur as chemical intermediates of pesticides such as permethrin. Carbon isotope fractionation of the three DCB isomers was investigated during anaerobic reductive dehalogenation, and the results showed large isotope fractionation of 1,3-DCB and 1,4-DCB, whereas only a small isotopic effect occurred for 1,2-DCB.<sup>92</sup> Therefore, a study on isotopic fractionation during the photolytic transformation of pyrethroids is still in its infancy and needs to be benchmarked against other processes such as biodegradation, and hydrolysis through the accumulation of CSIA techniques.

### Carbamates

Stable isotope analysis has been used to trace the source of methomyl,<sup>93</sup> as the degradation products of carbamate pesticides are generally non-toxic substances such as  $\text{NH}_4^-$ ,  $\text{SO}_4^{2-}$ , and  $\text{CO}_2$ . Isotopic fractionation during CSIA can be used to determine the type of reaction that triggers the degradation of a contaminant, specifically by describing the chemical bond changes in the reaction pathway. One reason why fewer photodegradation studies on CSIA have been conducted, compared to biodegradation or hydrolysis studies, is because photodegradation products can completely degrade into non-toxic and harmless substances. Thus, because carbamate pesticides are capable of complete mineralization under photodegradation conditions, unlike other types of pesticides, CSIA, as an assay technique based on tracking parent isotope fractionation, may pose some difficulties for CSIA studies.

Consequently, the photodegradation process needs to be prioritized before it can be measured. Furthermore, there are no studies related to CSIA and the photodegradation of carbamate insecticides. Thus, the photodegradation products and chemical bond changes of TBC have been well studied, so we can use TBC as a model substance for this class of pesticides to refine and optimize the photodegradation of CSIA technology.

### Phenoxyacetic acid derivatives

Substituted chlorobenzenes include many environmental contaminants such as the herbicides 2,4-D, dichlorprop, and chlortoluron.<sup>94</sup> However, the reaction mechanisms governing the direct and indirect photodegradation of substituted chlorobenzenes are not well understood. Therefore, studying the isotopic fractionation potentials during the photodegradation reactions of herbicide intermediates can help to determine the reaction pathways of herbicides during the photolysis process. Passeport *et al.*<sup>95</sup> studied only 4-nitrochlorobenzene and showed that the slow, but clear, isotope fractionation during direct photolysis was due to the pseudo first-order reaction rate as the constants increased according to the order of  $\text{NO}_2^- < \text{Cl}^- < \text{CH}_3^-$  substituted chlorobenzenes. The carbon enrichment factors in CSIA were traced during indirect photodegradation, which suggested that the rate-determining step in the reaction with OH radicals was the addition of the electrophile in the benzene ring. This resulted in the formation of O-chlorophenol and P-chlorophenol. Additionally, the substitution of OH radicals further attacking O-chlorophenol and P-chlorophenol proceeded at the *ortho* or *para* positions of the OH group. The detection of phenol intermediates in indirect photodegradation experiments with CMB isomers thus supported the preferential attack of OH radicals on the ring rather than the methyl group, which was consistent with the results of Zhang *et al.*<sup>5</sup> One study developed a new analytical method for <sup>37</sup>Cl-CSIA of MCB, and combined a chlorine isotope with <sup>13</sup>C-CSIA to estimate reductive dehalogenation during the biodegradation of MCB.<sup>96</sup> The data showed an enrichment factor of  $-0.6 \pm 0.1\%$  for <sup>37</sup>Cl. Thus, if differences in the values of Cl isotope enrichment factors are observed in the photodegradation process, this may suggest that CSIA can distinguish between aqueous photodegradation and other degradation processes.

### Other pesticides

Substituted anilines are a class of toxic and mutagenic environmental pollutants,<sup>97</sup> and they are widely used as intermediates in the manufacturing of pesticides,<sup>98</sup> such as alachlor, butachlor, and molinate. Skarpeli-Liati *et al.*<sup>99</sup> derived equilibrium isotope effects, specifically through enantiomer-specific stable isotope analysis (EIEs), and found that they were pertinent to the aromatic amine protonation of 0.980 and 1.001 for N and C, respectively. The values were similar for all compounds investigated. Stronger N–H bonds in protonated heavy nitrogen isotopologues of substituted anilines were due to the inverse N equilibrium isotope effects in a similar range. The fractionation associated with the protonation of aryl N atoms could potentially interfere with the quantification of N isotope fractionation



during contaminant transformation, if the latter involves reactions with N-containing functional groups. Thus, the magnitude of C and N isotope fractionation for the photodegradation processes of substituted anilines are currently unknown, and more research in this area is needed.

Another study tested the herbicide bentazone using an online methylation agent before isotope analysis, rather than gas GC-IRMS and LC-IRMS. The results showed that by using a higher trimethyl sulfonium hydroxide (TMSH) method to treat the analyte, the ratios produced appreciable reverse carbon and nitrogen isotope fractionation.<sup>100</sup> Consequently, carbon and nitrogen CSIA corroborated<sup>101</sup> the transformation of bentazone with significant enrichment of <sup>13</sup>C and <sup>15</sup>N. Carena *et al.*<sup>102</sup> showed that direct photolysis was the main photolytic pathway for bentazone in natural water samples, and the results were consistent with those of Katagi.<sup>103</sup> Understanding the link between CSIA and direct photolysis would therefore help demonstrate degradation, persistence, and source identification at various temporal and spatial scales.

Bromoxynil is a nitrile herbicide used to control annual broadleaved weeds. During photodegradation processes, dual isotope effects and  $\delta^{13}\text{C}$  and  $\delta^{15}\text{N}$  enrichment trends differed from  $\epsilon_{\text{C}} = 4.74 \pm 0.82\text{‰}$  and  $\epsilon_{\text{N}} = 0.76 \pm 0.12\text{‰}$ , to  $\epsilon_{\text{C}} = 0.34 \pm 0.44\text{‰}$  and  $\epsilon_{\text{N}} = -3.70 \pm 0.30\text{‰}$ , respectively. This suggested different mechanisms for the two processes, specifically between laboratory conditions and natural conditions.<sup>43</sup> A comparison of the carbon and nitrogen isotope enrichment factors under natural and laboratory conditions revealed significantly different trends, suggesting different mechanisms for the two processes under laboratory and natural conditions. This also suggested that the bromoxynil molecule recombines back to its original state during the reaction, but the cause of further degradation was not determined. However, the values of carbon isotope enrichment factor under UV conditions were higher than those under natural light conditions, which may have been because the degradation mechanism of bromoxynil under the two conditions was different. Furthermore, in combination with the degradation mechanism, photolysis is presumed to be the direct excitation mechanism, and debromination of bromoxynil by homogeneous C–Br bond cleavage in the solvent cage generates a singlet radical pair under UV radiation. However, the nitrogen isotope effect is also inverse, and though it is unexplained why fractionation of the N isotope is sizable even though none of the five N atoms are directly involved in the reaction. Under natural light conditions, the reaction starts with the excitation of deprotonated bromoxynil molecules into a triplonid intermediate, which is also reflected by the normal nitrogen isotope effect  $\epsilon_{\text{N}} = (-3.7 \pm 0.3)\text{‰}$ . This indicates that the intermediate is further converted to a bromoxynil free radical and then delocalized on the aromatic ring C≡N. Insignificant carbon isotopic fractionation may also result from multiple effects in the transition state, and cancel each other out, including the weakening of the C–Br bond and formation of a C=O, or “isotopic dilution” with nonreactive carbon.<sup>104,105</sup> Although hydrogen and bromine elements have not been incorporated into the current CSIA analytical methods for the photolytic analysis of bromobenzonitrile, further

developments could determine the isotopic effects of these elements and result in a more in-depth mechanistic analysis. The identical trends in isotopic values are obtained for both bromoxynil and atrazine<sup>34</sup> after photodegradation by CSIA, it can be assumed that the reaction mechanism have some similarity, and it is speculated that the bromobenzonitrile molecules may have recombined back to their original state during the reaction, but the cause of further degradation was not identified.

Chloroanilines can directly synthesize the insecticide diflubenzuron and can synthesize parachlorophenylurea or *p*-chlorobenzene isocyanate, which are two types of diflubenzuron insecticide intermediates. Ratti *et al.*<sup>31</sup> observed chloroaniline with different substituents for the variation of C and N isotope enrichment factors,  $\epsilon_{\text{C}}$  and  $\epsilon_{\text{N}}$ , between  $-1.2 \pm 0.2\text{‰}$  to  $-2.7 \pm 0.2\text{‰}$  for C, and  $-0.6 \pm 0.2\text{‰}$  to  $-9.1 \pm 1.6\text{‰}$  for N. The direct photodegradation of chloroaniline was very sensitive to changes in solution pH and ionic composition. The results also showed that the initial concentration of 4-Cl-aniline did not significantly affect the carbon isotope fractionation process during photolysis, but the carbon isotope enrichment factor changed from  $-1.2 \pm 0.2\text{‰}$  to  $+1.0 \pm 0.3\text{‰}$  with increased initial concentration. Coupling with another equivalent substrate also leads to an enrichment of nitrogen isotopes, and different pH conditions exhibit different reaction mechanisms. Specifically, 4-chloroaniline and reactive intermediates below pH 5 are unfavourably protonated, producing coloured coupling products, which introduce carbon isotope enrichment factors of different magnitudes and positive or negative magnitudes. In the direct photolysis study of atrazine and bromoxynil, the photophysical process of the excited state caused the depletion of isotopes, however, this has not been verified. Moreover, the photophysical process of the excited state was proven *via* the direct photolysis discussion of chloroaniline. With the addition of the quencher CsCl, the values of  $\epsilon_{\text{C}}$  and  $\epsilon_{\text{N}}$  have increased to varying degrees. This is because quencher CsCl, as a singlet quencher, decreases the lifetime of excited singlet states *via* increased intersystem-crossing, and thus increases excited triplet state formation. The results indicated that the fractionation of C and N isotopes is affected by the excited state of 4-Cl-aniline dechlorination, which may determine the reactivity factor. The  $\epsilon_{\text{C}}$  for 2-Cl-aniline photolysis ( $1.3 \pm 0.1\text{‰}$ ) notably differs from 4-Cl-aniline,<sup>31</sup> which may be interpreted as evidence for increased bonding to C in the rate-limiting step of the reaction. In conclusion, by comparing the AKIE isotopic values at different substitution sites, we can use the AKIE values to identify the isomers in which photodegradation occurs, and we can speculate on the mechanism of degradation for different species. These data suggest that the photophysical processes contribute to, or at least determine, the isotopic effect and isotopic fractionation associated with the photolysis of organic compounds. These results are difficult to rationalize based on bond cleavages, though the conclusions are consistent with the direct photolysis of atrazine.<sup>34</sup> However, it is more difficult to rationalize the isotope effects from photophysical processes because of the sensitivity of excited-state populations, different excited spin states, and the intersystem



crossing to isotopic substitution. Notably, this analysis can also be observed in the photochemical dechlorination of chloroanilines.<sup>13</sup>

Phenylurea herbicides are of environmental concern because they are often detected at concentrations above the legal threshold in soil and water.<sup>106</sup> Abiotic degradation of phenylurea herbicides are typically low, but they undergo different types of chemical transformations through a variety of processes, including photodecomposition. Isoproturon (IPU), 3-(4-isopropylphenyl)-1,1-dimethylurea, is a systemic non-biodegradable herbicide that acts as a photosynthesis inhibitor. The photocatalytic degradation of IPU<sup>107</sup> was studied in the presence of natural iron oxide, oxalic acid, and under UV irradiation. A recent study described the enhanced degradation of IPU by solar light in aqueous systems in the presence of TiO<sub>2</sub>, as well as diuron,<sup>108,109</sup> linuron,<sup>110</sup> monolinuron,<sup>111</sup> chlorotoluron,<sup>112</sup> monuron,<sup>113</sup> fenuron,<sup>114</sup> fluometuron,<sup>115</sup> and their main metabolites. Although the phototransformation process may contribute to the degradation of IPU, biodegradation appears to be the main phenomenon responsible for its natural attenuation in the environment. This appears to be also true for the other phenylureas, and CSIA is often used in biotransformation<sup>42</sup> reactions of IPU. Recent studies<sup>40,41</sup> have developed a GC-based method to make IPU accessible to carbon and nitrogen isotope analyses. They have also introduced CSIA to obtain additional information regarding the photochemical degradation mechanisms of isoproturon and methylamine. Furthermore, the observed indirect photodegradation studies of atrazine and 2-Cl-aniline may be related to the isotope's nuclear magnetic moment/spin. However, based on the information available so far, it is not possible to make a determination. Furthermore, the specific process leading to the inverse enrichment phenomenon in the photodegradation of isoproturon is described.<sup>40</sup> Normal heavy isotope enrichment occurs during the reaction, but the degree of C isotope fractionation during indirect photodegradation induced by nitrate is low, resulting in a relatively low enrichment factor  $\epsilon_C = -0.002 \pm 0.001\text{‰}$ , in contrast to direct photodegradation  $\epsilon_C = -0.018 \pm 0.006\text{‰}$ . This observed difference in values is due to two reasons. The carbon isotope fractionation effect is related to the mass of the other bonding element. Analysis of the degradation mechanism shows that the bond broken by demethylation of IPU in direct photolysis is the C–N bond, while the bond broken by isopropyl hydroxylation in indirect photolysis is the C–C bond. However, the C-atom reaction during the degradation of isoproturon does not necessarily occur at the active site, resulting in the dilution of the C-rich factor in the end. It is also possible that the carbonyl C of isoproturon and the N of dimethylamine are the two reactive atoms whose breakage leads to the primary carbon and nitrogen isotopic effects. In addition, the secondary isotopic effects occur at the terminal nitrogen and the two methyl carbons, specifically, the reaction of the isopropyl chain does not cause C stable isotopic fractionation. In contrast to the C stable isotope, the N stable isotope maintained stable retrograde fractionation under direct photodegradation ( $\Delta = -12.6615 \pm 1.2\text{‰}$ ), with normal C and anti-N isotope fractionation. This is typical of the oxidation reaction

and is characteristic of substituted aniline, suggesting that the phenomenon of N stable isotopes maintaining retrograde fractionation at later stages of degradation is related to the oxidation reaction of isopropyl substituted aniline. Although the key step of urea hydrolysis is breaking of the C–N bond, which leads to N stable isotope fractionation, it is still consistent with the bond breaking process that occurs during biodegradation. Nevertheless, the degree of stable isotope fractionation differs (Table 1), probably due to the slow translational degradation of organic substrates by microorganisms, whereas photodegradation is a relatively rapid process in which the organic molecules are directly converted by light energy. The difference in stable isotope fractionation between different degradation pathways is not only related to the reaction mechanism of different degradation pathways, but also to the specific degradation conditions. Jin and Rolle<sup>116</sup> proposed a mechanism-based modeling approach to simulate the degradation of IPU. Their model can be used to explore the phototransformation pathways in scenarios for which position-specific isotope data are unavailable. The Kubelka–Munk model can also be used for the photochemical study of carbaryl.<sup>117</sup>

Polychlorinated phenols are widely used as fungicides.<sup>118</sup> Research has focused on sources and transformations of polychlorinated phenols with the use of Cl<sup>−</sup> and C-CSIA.<sup>119</sup> The determined AKIE values have provided mechanistic insights regarding reaction mechanisms. Stable carbon isotopes have been coupled with dechlorination and soil redox of pentachlorophenol, revealing the mechanism of biochemical processes.<sup>120</sup> Therefore, the use of CSIA to study this substance has a high potential and operational basis. The former study also demonstrated the benefits of 2D CSIA compared to one-element CSIA for assessing the sources and transformations of environmental contaminants.

Chlorinated solvents, such as 1,1,1-trichloroethane (1,1,1-TCA) and 1,1,2-trichloroethane (1,1,2-TCA), have been widely used as chemical intermediates of insecticides, and they are found in groundwater. Broholm *et al.*<sup>121</sup> used carbon isotopes and CSIA to identify an alternative pathway, which cannot be explained by assuming biotic reductive dechlorination. In addition, single element kinetic isotope effects do not provide conclusive information about the reaction mechanism. During the biodegradation of 1,1,2-trichloroethane (1,1,2-TCA),<sup>122</sup> the AKIEs that were expected to cleave a C–Cl bond exhibited masking of the intrinsic isotope fractionation. Thus, a dual-element approach can reduce interpretation bias due to isotope-masking effects, and overcome the limitations to reveal the actual mechanism. However, neither of these studies mentioned photodegradation.

Newly produced pesticides will likely have superior performance compared to existing pesticides. For example, fluzaindolizine<sup>123</sup> is a new, highly effective, and selective nematicide, and data on the degradation of fluzaindolizine are currently limited.<sup>124</sup> The photodegradation kinetics of fluzaindolizine in aqueous solutions indicate a possible direct photolysis mechanism for fluzaindolizine. In addition, some direct transformation products have resulted from a series of



photochemical reactions involving ring-opening and oxidation, and have a high potential of being detected by CSIA.

For some pesticide types, such as arsenicals, bipyridylum derivatives, pyrazoles, copper compounds, coumarin derivatives, mercury compounds, and nitrophenol derivatives, no relevant research related to photodegradation and CSIA has been reported.

## Future outlook and challenges

The development and establishment of CSIA technology with more elements will broaden its potential for studying organic pollutants. CSIA technology also requires the integration of different elements for multi-dimensional analysis, so that the traceability results of organic pollutants are more accurate. Multi-element stable isotope analysis can be used for source identification, characterization, and identification of degradation mechanisms. Thus, it would be particularly useful for contaminant accumulation,<sup>125</sup> source detection,<sup>126</sup> and the development of regulatory and monitoring strategies.<sup>127</sup> As additional elements, such as <sup>2</sup>H,<sup>37,128</sup> <sup>37</sup>Cl,<sup>129</sup> and <sup>34</sup>S,<sup>130</sup> are included in the isotopic analysis of atrazine and its metabolite desethylatrazine in a given transformation process, the opportunity to assess the underlying reaction mechanism(s) increases.<sup>131</sup> This is particularly important for the photo-transformation processes of agrochemicals, where different functional groups or bonds of a molecule might be involved. For example, chlorine isotope fractionation could also be a sensitive indicator of even limited degradation, and Cl-CSIA is a promising tool for assessing the transformation process of acetochlor and metolachlor.<sup>132</sup> The methods validated in this study are therefore an important step toward accurate and precise Cl-CSIA of extracts, in the mg l<sup>-1</sup> concentration range in aquatic systems. For a given element that exists in a covalent bond with a comparable force constant, the isotopic effect tends to be greater if the element is bonded to a heavier atom. For example, the carbon isotopic effect is typically greater in C–O or C–Cl bond breaks, rather than in C–H bond breaks, and thus chlorine isotopes can characterize the breaking of C–Cl bonds. Even when degradation is limited, chlorine isotopes can still be used as sensitive indicators of the conversion process due to their strong fractionation. This information, combined with carbon and nitrogen isotope data, may be useful in laying the groundwork for understanding the photolytic reaction mechanism and quantifying the degradation mechanism of pesticides in the field. Lihl *et al.*<sup>133</sup> discussed the compound-specific standards of acetochlor and S-metolachlor enriched in <sup>37</sup>Cl/<sup>35</sup>Cl. The researchers emphasized the need for chlorine isotope standards that encompass a wider range of isotopic values to ensure accurate results and provide a basis for accurate chlorine CSIA. Yankelzon *et al.*<sup>134</sup> presented a benchmark for the routine application of Br–Cl-CSIA of micropollutants with numerous carbon atoms, Br, and Cl. This would allow it to be used for newer classes of contaminants, such as chlorinated pesticides. CSIA technology measures the stable isotope ratio of the target element of the target compound, and the results are not disturbed by other reactants, products, and elements. Two-

dimensional monomer isotope analysis (2D-CSIA) technology can be used to analyse the isotopes of two elements. In addition to the isotopic enrichment factors,  $\delta_E$  represents the elemental E isotopic composition of the residual parent reactant at some point in the reaction, and  $\Delta\delta^2\text{H}$ ,  $\Delta\delta^{15}\text{N}$ , and  $\Delta\delta^{13}\text{C}$  represent the relative  $\delta^{13}\text{C}$ ,  $\delta^2\text{H}$ , and  $\delta^{15}\text{N}$  excursions during the reaction. In previous reports,<sup>127,135,136</sup> isotopes or CSIA technology have mainly been used to determine  $\delta^{13}\text{C}$  and other isotopic  $\delta$  values of monomeric organic substances, removal efficiencies, and pesticide residues. Researchers have compared the isotopic effects of two elements plotted separately relative to each other,<sup>37</sup> creating two-element isotope plots, with different slopes reflecting the isotopic effects of different underlying mechanisms. Two-element isotope plots have the advantage of being insensitive to masking, and if there are other rate-limiting steps in the reaction, such as the binding of enzymes to substrates during biodegradation, the apparent isotopic kinetics that are observed may be greatly reduced.<sup>16</sup> The slope of the two-element isotope diagram remains constant because the KIE fluxes of the two elements usually decrease in equal proportions. In addition, this representation may also apply to hydrolysis reactions at different pHs, making it easier to distinguish between different types of hydrolysis processes because of the positive and negative values of the slope.<sup>81</sup> However, this analysis may also have its shortcomings due to the small number of elements. In direct and indirect photodegradation studies atrazine,  $\Delta\delta^2\text{H}/\Delta\delta^{13}\text{C}$ ,  $\Delta\delta^2\text{H}/\Delta\delta^{15}\text{N}$ , and  $\Delta\delta^{15}\text{N}/\Delta\delta^{13}\text{C}$  were correlated. Although characteristic carbon and nitrogen isotope patterns emerged, the differences were small and similar to the slopes of the transformation pathways that yielded the same products. Furthermore, the values of the slopes could not be used to determine the main reaction sites of the two photo-oxidant reactions.<sup>35,131</sup> These data therefore show that specific isotopes in molecules become “fingerprints”, indicating the source of trace organic pollutants in the environment. When the composition changes (C–H, C–N, C–Cl), the effects of catalytic stress on isotopic fractionation are effectively eliminated, and the reliability and the accuracy of the results will improve.<sup>137</sup>

The CSIA approach is commonly based on the KIEs, where the chemical bonds of lighter isotopes are cleaved slightly faster than the bonds on heavier isotopes. This leads to the enrichment of the residual non-degraded fraction in the heavier isotopes. Dual-element isotope enrichment has been established for identifying the degradation mechanism. Usually, several atoms of a given element are present at various positions in a larger organic molecule. For this element, isotopically graded separation is only possible at the positions where the covalent bonds of the element are broken or formed, either directly or indirectly, in a given rate-limiting step. Thus, many isotopes are not directly involved in the reaction, and the volume enrichment factor becomes smaller due to the “dilution” effect of the non-reactive isotopes. To address the variability of the enrichment factors, a large amount of isotopic fractionation data are converted to site-specific AKIEs. The element with the largest relative mass difference between the light and heavy isotopes will obtain the highest fractionation, and the hydrogen isotope effect is often much larger than the





carbon isotope effect. The  $^{13}\text{C}$ - and  $^{15}\text{N}$ -AKIE of 4-Cl-aniline<sup>30</sup> are greater than 1.010 and 1.002, respectively, and can be used to effectively distinguish isotopic fractionation under different excited state conditions. In contrast, 3-chloroaniline is subject to rate-limiting photophysical processes, with little change in C isotopic composition and minor N isotopic fractionation, which also suggests that photophysical processes may contribute to, or even determine, isotopic effects. However, if KIE does not have known reference data,<sup>138</sup> the observed AKIE may occasionally be considerably smaller. This may occur when the bond conversion involving the measured element and representing the rate determining step of the whole process is preceded by a process that is either not fractionated, or only slightly fractionated, such as adsorption to a reactive surface, before the actual transformation. In the indirect photodegradation reaction of atrazine, AKIE<sub>H</sub> values are smaller when hydroxyl radicals are used as photooxidants, and may be due to the near diffusion control of the reaction rate in this system, as well as the masking of the  $^2\text{H}$  isotopic effect. In addition, the magnetic moment or nuclear volume in the nucleus of an isotope may change, causing a non-atomic mass-dependent isotopic fractionation effect. During photodegradation, a number of factors result in an isotopic fractionation pattern that is more difficult to analyse. For example, the direct photodegradation isotope depletion of atrazine may result mainly from the magnetic isotope effect of photophysical processes. Thus, isotopic effects from photophysical processes are more difficult to rationalize and may be more variable, as they depend on the population and reactivity of different excited spin states. Research on the degradation mechanism of organic matter is thus insufficient. The use of CSIA in the traceability of pesticide residues provides valuable information. However, using CSIA to identify pesticide photodegradation mechanisms requires further research.

During CSIA, some methods that are used during sample pretreatment, testing, and analysis can be combined, giving researchers a basis for systematic evaluation and identification of isotopic fractionation and degradation pathways (Table 2). The combination of CSIA and large volume extraction makes it possible to measure herbicide and metabolite mixtures in the natural environment, with the pre-treatment of carbon and nitrogen isotopes with high accuracy and feasibility.<sup>139</sup> During testing, high temperature conversion (HTC) enables the direct pyrolysis of organically bound hydrogen elements into hydrogen analysis gas, thus facilitating hydrogen-containing compound-specific isotope analysis (CSIA) and optimizing the CSIA-H test method. This method is challenging for organics that contain nitrogen, chlorine and sulphur, as the Cr-based reactor system (Cr/HTC) can overcome interference by quantitative removal of heteroatoms due to the presence of hydrogen by-products.<sup>28</sup> Thus, gas chromatography (GC) coupled with mass spectrometry (GC-MS) has been applied to CSIA. The CSIA-Cl/Br method that uses GC-quadrupole MS (GC-qMS) significantly simplifies sample pretreatment,<sup>140</sup> but asymmetric and/or broad peaks that appear during analysis, making it difficult to accurately integrate peak areas, which affects the accuracy of CSIA results. Gas chromatography/isotope ratio mass spectrometry (GC-IRMS) is limited to the analysis of certain

compounds and molecular fragments by fixed Faraday detector alignments. Modern CSIA techniques using multiple collector-inductively coupled plasma MS (MC-ICPMS), in combination with gas chromatography (GC-MC-ICPMS), are orders of magnitude more accurate and therefore more commonly used for chlorine isotope analysis. Although previous applications were limited to volatile organic matter (VOCs), instrument setup and sample handling methods have improved to include the detection of semi-VOCs.<sup>141</sup> Gas chromatography-electron ionization-mass spectrometry (GC-EI-MS) can reveal the degradation of halogenated organic compounds. Chemical bonds that are cut or formed in EI-MS can cause both intramolecular and intermolecular isotope effects, and these inherent limitations of GC-EI-MS may trigger uncertainty and bias in CSIA-Cl/Br results. GC-DFS-HRMS and GC-HR-TOF MS have been discussed previously.<sup>69</sup> In GC-MS quantitative analysis, quantitative results are adversely affected by a phenomenon known as the “matrix effect”.<sup>147</sup> Also, isotopic fractionation may occur on a gas chromatography column, or on the entire gas chromatography system, which is inherent to GC and may lead to biased CSIA results. Due to the different boiling points and thermal sensitivities of some pesticides, such as semi-volatile pesticides, liquid chromatography rather than gas chromatography in combination with mass spectrometry may be used for the analysis of photodegradation processes. For example, ultra-liquid chromatography can be coupled with quadrupole time-of-flight mass spectrometry (UHPLC-Q-TOF/MS)<sup>142</sup> or HPLC-Qtof-MS.<sup>143</sup> Research<sup>142</sup> has shown that  $\delta^{13}\text{C}$  and  $\delta^{15}\text{N}$  of CSIA for non-volatile compounds can be detected by high-performance liquid chromatography/isotope ratio mass spectrometry (HPLC/IRMS). Other detection techniques and models may be used to validate or supplement the photolytic or biodegradation processes of pesticides that cannot be explained directly by CSIA, such as the occurrence of inverse isotope fractionation. By combining different techniques, we can verify if there is a different degradation mechanism, or if it is due to an error in the instrument itself. For example,  $^1\text{H}$  NMR spectroscopy can determine the identity of the intermediates and products obtained upon UV-A photolysis, and has determined that benzamide is the major final photoproduct of azinphos-methyl.<sup>148</sup> Christian *et al.*<sup>144</sup> also illustrated the applicability of  $^1\text{H}$  NMR spectroscopy in the kinetic investigation and hydrolysis of dichlorvos. More importantly, quantitative deuterium nuclear magnetic resonance (NMR) spectroscopy can quantitatively determine the  $^2\text{H}/^1\text{H}$  ratio in the active group of the reactants and compare it with the  $^2\text{H}/^1\text{H}$  ratio measured by isotope ratio mass spectrometry (GC/IRMS) applied in CSIA technology to verify the authenticity of the  $\delta^2\text{H}$  value. The stable isotope probing (SIP) technique is applied to the differences in the community structure of microorganisms during microbial degradation of organic matter, and can provide a complementary description of microbial population types for the biodegradation CSIA analysis process.<sup>145</sup> The fate of commonly used herbicides, such as flufenacet and metazachlor, along with the ecohydrological Soil and Water Assessment Tool (SWAT model),<sup>146</sup> have been used to test the applicability of these pesticides. In the SWAT model, pesticides are represented by

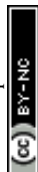


Table 2 Some technical methods that can be used to assist compound-specific isotope analysis (CSIA)<sup>a</sup>

Methods	Category	Remarks (CSIA method or photodegradation development)	Reference
Solid-phase extraction (SPE)	Pre-treatment	Extraction conditions, including the nature and volume of the elution solvent, the amount of sorbent, and the solution pH were optimized	Torrentó <i>et al.</i> <sup>139</sup>
High-temperature conversion (HTC)	Test	Direct pyrolysis of organically bound hydrogen into hydrogen gas for analysis	Wu <i>et al.</i> <sup>28</sup>
Chromium-based HTC (Cr/HTC)	Test	Chromium-based reactor systems can eliminate interference from impurities by quantitatively removing heteroatoms	Wu <i>et al.</i> <sup>28</sup>
GC-quadrupole MS (GC-qMS)	Analysis	Continuous flow analysis of non-combustible molecules of the substance to be measured; analysis and elimination of influencing factors for the quantitative analysis of chlorine isotopes, such as different instruments and detection times	Bernstein <i>et al.</i> <sup>140</sup>
Gas chromatography (GC-MC-ICPMS)	Analysis	Method for compound-specific chlorine isotopic analysis of volatile organics and some semi-volatile organics and GC-MC-ICPMS is nearly one order of magnitude more precise and universal and is straight forward to calibrate	Renpenning <i>et al.</i> <sup>141</sup>
Gas chromatography-electron ionization-mass spectrometry (GC-EI-MS)	Analysis	GC-EI-MS can cut and form chemical bonds while producing intra- and intermolecular isotopic effects, which in turn can bias CSIA results	Tang <i>et al.</i> <sup>69</sup>
GC double focusing magnetic sector high-resolution mass spectrometry (GC-DFS-HRMS)	Analysis	CSIA results are also influenced by peak retention time and peak shape	Tang <i>et al.</i> <sup>68,69</sup>
High-performance liquid chromatography/isotope ratio mass spectrometry (HPLC/IRMS)	Analysis	$\delta^{13}\text{C}$ and $\delta^{15}\text{N}$ of CSIA of non-volatile compounds can be detected	Sivaperumal <i>et al.</i> , <sup>142</sup> Sandín-España <i>et al.</i> <sup>143</sup>
<sup>1</sup> H NMR spectroscopy	Verified method	Comparison of the measured <sup>2</sup> H/ <sup>1</sup> H ratio verifies the validity of the calculated $\delta^2\text{H}$ values from CSIA analysis	Christian <i>et al.</i> <sup>144</sup>
Stable isotope probing (SIP)	Verified method	Identify the differences in the community structure of microorganisms during microbial degradation	Jiang <i>et al.</i> <sup>145</sup>
Soil and Water Assessment Tool (SWAT model)	Model	Test applicability for use with flufenacet and metazachlor	Fohrer <i>et al.</i> <sup>146</sup>
Bioavailability (BA)	Model	$\text{BA} = 1 - \frac{b}{c_0 \times [(1 + \delta_i^{13}\text{C}) / (1 + \delta_0^{13}\text{C})]^{1/\epsilon}}$	Xu <i>et al.</i> <sup>53,54</sup>

<sup>a</sup> The physical quantities listed in the BA formula are marked in the ESI (see ESI).

one constant value for each parameter and are not adjusted according to changing environmental conditions. CSIA technology may also be used with enantioselective analysis to evaluate the degradation extent and mechanisms of chiral pesticides in the soil. In the analysis of pesticide degradation processes by CSIA, the calculation results and the speculation of the degradation mechanism are often validated by chemical models. In the CSIA enrichment factor or apparent kinetic constant evaluation process, simplified kinetic models are used to assess the degradation kinetic constants or the influence of factors such as pH on the degree of degradation.<sup>31</sup> Bioavailability models can also be used to reflect the rate at which contaminants enter the body from the food chain during CSIA testing.<sup>53,54</sup> Chemical calculation models such as the relative change in isotopic ratio between reactants and products ( $\Delta hE$ ) can also be used to characterize the magnitude and direction of fractionation when testing the accuracy and sensitivity of the instrument.<sup>69</sup> ESIA, which combines two approaches—enantiospecific concentration analysis and CSIA—provides

information on <sup>13</sup>C/<sup>12</sup>C ratios. This method was applied to the insecticide  $\alpha$ -hexachlorocyclohexane,<sup>33</sup> and studies<sup>38,149</sup> have provided a method for investigating the biodegradation of three polar pesticides, specifically 4-CPP ((RS)-2-(4-chloro-phenoxy)-propionic acid), mecoprop (2-(4-chloro-2-methyl-phenoxy)-propionic acid), and dichlorprop (2-(2,4-dichlorophenoxy)-propionic acid), or the biodegradation of the chiral fungicide metalaxyl. Accordingly, the results indicated that hydroxylation is the major enantioselective degradation pathway in soils. Thus, ESIA has the potential to distinguish enantiomer degradation from non-destructive dissipation.

## Conclusions

CSIA can be used to evaluate *in situ* pesticide degradation and estimate independent pesticide degradation procedures.<sup>13</sup> Reference  $\epsilon$  values for specific abiotic transformation mechanisms of pesticides have been obtained from laboratory experiments.<sup>34,150</sup> These results quantify the isotopic composition at



the mechanistic level and provide an additional and sometimes the only means for identifying and quantifying the transformation reactions of organic compounds.<sup>151</sup> However, there have been improvements such as multi-element stable isotopes of existing analytical methods for chlorine and hydrogen CSIA.<sup>152</sup> C–N isotope dual plots derived from photodegradation may help to separate photodegradation effects from other pesticide dissipation pathways.<sup>38</sup>

Based on the reviews provided for each category of pesticides using CSIA, we summarize some of the main findings below.

(1) Carbon stable isotope and nitrogen stable isotope fractionation enrichment factors under different photolysis pathways for the same pesticide can vary widely, indicating that the differences in reaction mechanisms due to different reaction pathways can affect product formation and thus fractionation and enrichment. The differences can also explain the reaction mechanisms of direct photodegradation, and indirect photolysis can be verified by the fractionation results of stable isotopes.

(2) The values of carbon stable isotope enrichment factors for different pesticides under the same photolysis pathway exhibited large differences in both normal and inverse values, indicating that different reaction sites, formation groups, and the degree of reactive degradation of the photodegradation process differed among the pesticides, depending on KIE or MIE. Nitrogen stable isotope fractionation and enrichment factors have been measured for some pesticides (chloroaniline, atrazine, isoproturon, and bromoxynil) but not for others, depending on whether nitrogen-containing groups were involved in the reaction and the content of the nitrogen-containing groups.

(3) The differences in the stable isotope concentration coefficients may be due to differences in the mass of other elements bound to the reacting atoms during photodegradation, or due to dilution by heavy isotopes of the same species but not in the active site. It is also possible that the secondary isotope effect is the determining step for the stable isotope enrichment factor.

(4) In pesticide photodegradation studies, the most commonly used stable isotopes are carbon and nitrogen. In addition to the widely used carbon isotopes, isotopes such as oxygen and hydrogen have received special attention, depending on the maturity and accuracy of the detection technology.

(5) Stable isotope enrichment factors for pesticides undergoing photodegradation are numerically different from other types of degradation processes (Table 1). This indicates that it is possible to use stable isotopes to effectively identify photodegradation pathways with other degradations. However, because CSIA does not require the determination of degradation products, by-product studies need to be integrated into the analysis. Other techniques, such as HTC, SIP, <sup>1</sup>H NMR spectroscopy, and the chemical model, may also be used (Table 2).

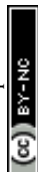
## Abbreviation index

AKIE	Apparent kinetic isotope effect
AKIEC	Apparent kinetic carbon isotope effect

AMPA	Aminomethylphosphonic acid
CSIA	Compound specific isotope analysis
CSIA-Cl/Br	Compound-specific chlorine/bromine isotope analysis
DCBs	Dichlorobenzenes
DDD	1-Chloro-4-[2,2-dichloro-1-(4-chlorophenyl)ethyl]benzene
DDE	1,1-Bis-(4-chlorophenyl)-2,2-dichloroethene
DDT	Dichloro-diphenyl-trichloroethane
EI-MS	Electron ionization mass spectrometry
GC/IRMS	Gas chromatography/isotope ratio mass spectrometry
GC/MS	Gas chromatography/mass spectrometry
GC-C-IRMS	Gas chromatography-combustion-isotope ratio mass spectrometry
GC-DFS-HRMS	GC bifocal sector high-resolution mass spectrometry
GC-EI-MS	Gas chromatography EI-MS
GC-HR-TOF-MS	Gas chromatography-high resolution time-of-flight mass spectrometry
GC-IRMS	Gas chromatography-isotope ratio mass spectrometry
GC-MC-ICPMS	Gas chromatography interfaced with multiple-collector inductively coupled plasma mass spectrometry
GC-MS	Gas chromatography-mass spectrometry
HCB	Hexachlorobenzene
HCHs	Hexachlorocyclohexanes
HPLC	High-performance liquid chromatography
HTC	High-temperature conversion
IPU	Isoproturon
LC-MS	Liquid chromatography-mass spectrometry
MET	Methomyl ( <i>S</i> -methyl- <i>N</i> -(methylcarbamoyloxy)thioacetimide)
OPs	Organophosphorus
SIP	Stable isotope probing
SPE	Solid phase extraction
SWAT	Soil and water assessment tool
TBC	Thiobencarb ( <i>S</i> -4-chlorobenzyl diethyl thiocarbamate)
TCEP	Tris(2-carboxyethyl)phosphine
TMSH	Trimethyl sulfonium hydroxide
UHPLC-Q-TOF/MS	Liquid chromatography coupled with quadrupole time-of-flight mass spectrometry
UPLC-MS-MS	Ultra-performance liquid chromatography-tandem mass spectrometry
USE	Ultrasound assisted extraction
UV-OZ	Ultraviolet photolysis ozonation

## Author contributions

The manuscript was written through the contribution of all authors. All authors have approved the final version of the manuscript.



## Conflicts of interest

There are no conflicts to declare.

## Acknowledgements

We would like to thank the anonymous reviewers and the associate editor for their comments, which improved the manuscript. We would like to thank LetPub (www.letpub.com) for providing linguistic assistance and scientific consultation during the preparation of this manuscript. This work was supported by the Key Program of China (2018YFC1803103, 2017ZX07206) and the National Natural Science Foundation of China (No. 21377098). The funders had no role in the study design, collection, analysis, or interpretation of the data, writing of the manuscript, or in the decision to submit the article for publication.

## Notes and references

- J. Varma and N. Dubey, *Curr. Sci.*, 1999, **76**, 172–179.
- World Health Organization, *The WHO Recommended Classification of Pesticides by Hazard and Guidelines to Classification 2009*, World Health Organization, 2010.
- B. S. Choudri and Y. Charabi, *Water Environ. Res.*, 2019, **91**, 1342–1349.
- W. Zhang, F. Jiang and J. Ou, *Proc. Int. Acad. Ecol. Environ. Sci.*, 2011, **1**, 125–144.
- W. Zhang, Y. Qi and Z. Zhang, *Environ. Monit. Assess.*, 2006, **119**, 609–620.
- M. C. Alavanja, J. A. Hoppin and F. Kamel, *Annu. Rev. Public Health*, 2004, **25**, 155–197.
- K. L. Bassil, C. Vakil, M. Sanborn, D. C. Cole, J. S. Kaur and K. J. Kerr, *Can. Fam. Physician*, 2007, **53**, 1704–1711.
- C. N. Kesavachandran, M. Fareed, M. K. Pathak, V. Bihari, N. Mathur and A. K. Srivastava, in *Reviews of Environmental Contamination and Toxicology (Continuation of Residue Reviews)*, ed. D. Whitacre, Springer, Boston, MA, 2009, vol. 200, pp. 33–52.
- J. Aislabie and G. Lloyd-Jones, *Soil Res.*, 1995, **33**, 925–942.
- H. D. Burrows, L. M. Canle, J. A. Santaballa and S. Steenken, *J. Photochem. Photobiol., B*, 2002, **67**, 71–108.
- T. Katagi, in *Reviews of Environmental Contamination and Toxicology: Continuation of Residue Reviews*, ed. G. W. Ware, Springer, New York, NY, 2004, vol. 182, pp. 1–78.
- S. Sondhia, P. P. Choudhury and A. R. Sharma, *Herbicide Residue Research in India*, Springer, Singapore, 2019.
- M. Elsner, *J. Environ. Monit.*, 2010, **12**, 2005–2031.
- T. B. Hofstetter and M. Berg, *TrAC, Trends Anal. Chem.*, 2011, **30**, 618–627.
- M. Blessing, M. A. Jochmann and T. C. Schmidt, *Anal. Bioanal. Chem.*, 2008, **390**, 591–603.
- M. Elsner, L. Zwank, D. Hunkeler and R. P. Schwarzenbach, *Environ. Sci. Technol.*, 2005, **39**, 6896–6916.
- M. Elsner and G. Imfeld, *Curr. Opin. Biotechnol.*, 2016, **41**, 60–72.
- X. Li, X. Peng and Q. Zhang, *Period. Ocean Univ. China*, 2009, **39**, 1251–1256.
- M. Elsner, L. Zwank, D. Hunkeler and R. P. Schwarzenbach, *Environ. Sci. Technol.*, 2005, **39**(18), 6896–6916.
- T. Mchugh, T. Kuder, S. Fiorenza, K. Gorder, E. Dettenmaier and P. Philp, *Environ. Sci. Technol.*, 2011, **45**, 5952–5958.
- N. Boens, E. Novikov and M. Ameloot, *J. Phys. Chem. A*, 2008, **112**, 2738–2742.
- L. Wu, J. Yao, P. Trebse, N. Zhang and H. H. Richnow, *Chemosphere*, 2014, **111**, 458–463.
- R. Farooq, F.-K. Lin, Y. Wang, J.-J. Huang, Z. Xu and S. F. Shaikat, *J. Shanghai Univ.*, 2004, **8**, 221–226.
- T. Oncescu and P. Oancea, *Rev. Chim.*, 2007, **58**, 232–235.
- J.-J. Yao, M. R. Hoffmann, N.-Y. Gao, Z. Zhang and L. Li, *Water Res.*, 2011, **45**, 5886–5894.
- D. Wang, J. Chen and Y. Su, *Foshan Ceram.*, 2006, **16**, 1–3.
- L. Wu, B. Chladkova, O. J. Lechtenfeld, S. Lian, J. Schindelka, H. Herrmann and H. H. Richnow, *Sci. Total Environ.*, 2018, **615**, 20–28.
- L. Wu, S. Kümmel and H. H. Richnow, *Anal. Bioanal. Chem.*, 2017, **409**, 2581–2590.
- E. H. Sandy, R. E. Blake, S. J. Chang, Y. Jun and C. Yu, *J. Hazard. Mater.*, 2013, **260**, 947–954.
- M. Ratti, S. Canonica, K. McNeill, J. Bolotin and T. B. Hofstetter, *Environ. Sci. Technol.*, 2015, **49**, 9797–9806.
- M. Ratti, S. Canonica, K. McNeill, P. R. Erickson, J. Bolotin and T. B. Hofstetter, *Environ. Sci. Technol.*, 2015, **49**, 4263–4273.
- N. Zhang, S. Bashir, J. Qin, J. Schindelka, A. Fischer, I. Nijenhuis, H. Herrmann, L. Y. Wick and H. H. Richnow, *J. Hazard. Mater.*, 2014, **280**, 750–757.
- S. L. Badea, C. Vogt, M. Gehre, A. Fischer, A. F. Danet and H. H. Richnow, *Rapid Commun. Mass Spectrom.*, 2011, **25**, 1363–1372.
- A. E. Hartenbach, T. B. Hofstetter, P. R. Tentscher, S. Canonica, M. Berg and R. P. Schwarzenbach, *Environ. Sci. Technol.*, 2008, **42**, 7751–7756.
- J. A. Khan, X. He, N. S. Shah, H. M. Khan, E. Hapeshi, D. Fatta-Kassinos and D. D. Dionysiou, *Chem. Eng. J.*, 2014, **252**, 393–403.
- A. H. Meyer, PhD thesis, Technische Universität München, 2010.
- A. H. Meyer, A. Dybala-Defratyka, P. J. Alaimo, I. Geronimo and M. Elsner, *Dalton Trans.*, 2014, **43**, 12175–12186.
- J. Masbou, F. Meite, B. Guyot and G. Imfeld, *J. Hazard. Mater.*, 2018, **353**, 99–107.
- S. Chen, K. Zhang, R. K. Jha, C. Chen, H. Yu, Y. Liu and L. Ma, *Environ. Pollut.*, 2019, **248**, 857–864.
- H. Yu, J. Liu, C. Han, H. Fang, X. Shu, Y. Liu, Y. Pan and L. Ma, *Research Square*, 2020.
- H. Penning and M. Elsner, *Anal. Chem.*, 2007, **79**, 8399–8405.
- H. Penning, S. R. Sorensen, A. H. Meyer, J. Aamand and M. Elsner, *Environ. Sci. Technol.*, 2010, **44**, 2372–2378.
- N. Knossow, H. Siebner and A. Bernstein, *J. Hazard. Mater.*, 2020, **388**, 122036.





- 44 N. Zhang, J. Schindelka, H. Herrmann, C. George, M. Rosell, S. Herrero-Martín, P. Klán and H. H. Richnow, *Environ. Sci. Technol.*, 2015, **49**, 233–242.
- 45 Food and Agriculture Organization, [http://www.fao.org/fileadmin/templates/agphome/documents/Pests\\_Pesticides/JMPR/Evaluation03/Dimethoate\\_2003.pdf](http://www.fao.org/fileadmin/templates/agphome/documents/Pests_Pesticides/JMPR/Evaluation03/Dimethoate_2003.pdf), accessed 21 December 2020.
- 46 J. Liu, L. Wu, S. Kümmel, J. Yao, T. Schaefer, H. Herrmann and H.-H. Richnow, *Chemosphere*, 2018, **212**, 133–142.
- 47 K. McLaughlin, C. Kendall, S. R. Silva, M. Young and A. Paytan, *J. Geophys. Res.: Biogeosci.*, 2006, **111**, G03003.
- 48 J. R. O'Neil, T. W. Vennemann and W. F. McKenzie, *Geochim. Cosmochim. Acta*, 2003, **67**, 3135–3144.
- 49 Y. Zakon, L. Halicz and F. Gelman, *Environ. Sci. Technol.*, 2013, **47**, 14147–14153.
- 50 A. L. Buchachenko, *J. Phys. Chem. B*, 2013, **117**, 2231–2238.
- 51 V. N. Epov, D. Malinovskiy, F. Vanhaecke, D. Bégué and O. F. X. Donard, *J. Anal. At. Spectrom.*, 2011, **26**, 1142–1156.
- 52 X. Tang, Y. Yang, W. Huang, M. B. McBride, J. Guo, R. Tao and Y. Dai, *Bioresour. Technol.*, 2017, **233**, 264–270.
- 53 Z. Xu, X. Shen, X. C. Zhang, W. Liu and F. Yang, *J. Hazard. Mater.*, 2015, **295**, 37–42.
- 54 Z. Xu, W. Liu and F. Yang, *J. Hazard. Mater.*, 2018, **349**, 1–9.
- 55 H. Shemer and K. G. Linden, *J. Hazard. Mater.*, 2006, **136**, 553–559.
- 56 J. Zhao, Y. Jiang, M. Kong, G. Liu and D. D. Dionysiou, *J. Hazard. Mater.*, 2018, **358**, 319–326.
- 57 D. M. Kujawinski, J. B. Wolbert, L. Zhang, M. A. Jochmann, D. Widory, N. Baran and T. C. Schmidt, *Anal. Bioanal. Chem.*, 2013, **405**, 2869–2878.
- 58 E. O. Mogusu, J. B. Wolbert, D. M. Kujawinski, M. A. Jochmann and M. Elsner, *Anal. Bioanal. Chem.*, 2015, **407**, 5249–5260.
- 59 J. Vijgen, P. Abhilash, Y. F. Li, R. Lal, M. Forter, J. Torres, N. Singh, M. Yunus, C. Tian and A. Schäffer, *Environ. Sci. Pollut. Res.*, 2011, **18**, 152–162.
- 60 I. Nijenhuis, J. Andert, K. Beck, M. Kästner, G. Diekert and H.-H. Richnow, *Appl. Environ. Microbiol.*, 2005, **71**, 3413–3419.
- 61 N. Ivdra, S. Herrero-Martín and A. Fischer, *J. Chromatogr. A*, 2014, **1355**, 36–45.
- 62 N. Ivdra, A. Fischer, S. Herrero-Martín, T. Giunta, M. Bonifacie and H. H. Richnow, *Environ. Sci. Technol.*, 2017, **51**, 446–454.
- 63 S. Li, L.-Y. Zhang, X.-S. Wang, H.-Q. Ma, Y. Wang and Z.-J. Guan, *J. Jilin Univ., Sci. Ed.*, 2007, **45**, 159–163.
- 64 B. Yu, J. Zeng, L. Gong, M. Zhang, L. Zhang and X. Chen, *Talanta*, 2007, **72**, 1667–1674.
- 65 L. Niu, C. Xu, S. Zhu, H. Bao, Y. Xu, H. Li, Z. Zhang, X. Zhang, J. Qiu and W. Liu, *Sci. Rep.*, 2016, **6**, 38475.
- 66 L. Kang, Q.-S. He, W. He, X.-Z. Kong, W.-X. Liu, W.-J. Wu, Y.-L. Li, X.-Y. Lan and F.-L. Xu, *Environ. Pollut.*, 2016, **219**, 883–896.
- 67 H. Holmstrand, M. Mandalakis, Z. Zencak, P. Andersson and O. Gustafsson, *Chemosphere*, 2007, **69**, 1533–1539.
- 68 C. Tang, J. Tan, S. Xiong, J. Liu, Y. Fan and X. Peng, *J. Chromatogr. A*, 2017, **1514**, 103–109.
- 69 C. Tang, J. Tan, Z. Shi, Y. Fan, Z. Yu and X. Peng, *J. Chromatogr. A*, 2019, **1603**, 278–287.
- 70 S. Yamada, Y. Naito, M. Takada, S. Nakai and M. Hosomi, *Chemosphere*, 2008, **70**, 731–736.
- 71 X.-D. Liu, L. Li, Y. Chi and Z.-J. Zhang, *J. Chin. Mass Spectrom. Soc.*, 2016, **37**, 10–16.
- 72 S. Y. Sohn, K. Kuntze, I. Nijenhuis and M. M. Haggblom, *Chemosphere*, 2018, **193**, 785–792.
- 73 Q. Cheng, Q. Teng, S. A. Marchitti, C. M. Dillingham and J. F. Kenneke, *Chirality*, 2016, **28**, 633–641.
- 74 Q. Guan, R. Zheng, L. Liu, H. Huang, M. Kang and J. Lu, *Strait J. Prev. Med.*, 2017, **23**(3–5), 84.
- 75 J. Da Silva, A. Da Silva, I. Khmelinskii, J. Martinho and L. V. Ferreira, *J. Photochem. Photobiol., A*, 2001, **142**, 31–37.
- 76 M. Zhou, C. Wei, G. Sheng and T. Lu, *Chin. J. Environ. Eng.*, 2019, **13**, 810–817.
- 77 T. Chacko, D. R. Cole and J. Horita, *Rev. Mineral. Geochem.*, 2001, **43**, 1–81.
- 78 J. R. Rohr, A. M. Schotthoefer, T. R. Raffel, H. J. Carrick, N. Halstead, J. T. Hoverman, C. M. Johnson, L. B. Johnson, C. Lieske, M. D. Piwoni, P. K. Schoff and V. R. Beasley, *Nature*, 2008, **455**, 1235–1239.
- 79 E. Pelizzetti, V. Maurino, C. Minero, V. Carlin and O. Zerbini, *Environ. Sci. Technol.*, 1990, **24**, 1559–1565.
- 80 S. Sanches, M. T. B. Cresp and V. J. Pereira, *Water Res.*, 2010, **44**, 1809–1818.
- 81 J. Masbou, G. Drouin, S. Payraudeau and G. Imfeld, *Chemosphere*, 2018, **213**, 368–376.
- 82 J. M. Oliva, M. E. D. G. Azenha, H. D. Burrows, R. Coimbra, J. S. Seixas de Melo, M. Canle L., M. I. Fernández, J. A. Santaballa and L. Serrano-Andrés, *ChemPhysChem*, 2005, **6**, 306–314.
- 83 A. L. Buchachenko, *Chem. Rev.*, 1995, **95**, 2507–2528.
- 84 B. Wu, W. A. Arnold and L. Ma, *Water Res.*, 2021, **190**, 116659.
- 85 W. Liu and J. J. Gan, *J. Agric. Food Chem.*, 2004, **52**, 755–761.
- 86 S. Tuck, A. Furey, S. Crooks and M. Danaher, *Food Addit. Contam., Part A: Chem., Anal., Control, Exposure Risk Assess.*, 2018, **35**, 911–940.
- 87 S. W. Chung and C. Lam, *Anal. Bioanal. Chem.*, 2012, **403**, 885–896.
- 88 D. A. Koch, K. Clark and D. M. Tessier, *J. Agric. Food Chem.*, 2013, **61**, 2330–2339.
- 89 Q. Zhu, Y. Yang, Y. Zhong, Z. Lao, P. O'Neill, D. Hong, K. Zhang and S. Zhao, *Chemosphere*, 2020, **254**, 126779.
- 90 X. Shen, Z. Xu, X. Zhang and F. Yang, *Sci. Total Environ.*, 2015, **532**, 415–419.
- 91 S. Jin, X. Yao, Z. Xu, X. Zhang and F. Yang, *Environ. Sci. Pollut. Res. Int.*, 2018, **25**, 22736–22743.
- 92 X. Liang, S. O. Mundle, J. L. Nelson, E. Passeport, C. C. Chan, G. Lacrampe-Couloume, S. H. Zinder and B. Sherwood Lollar, *Environ. Sci. Technol.*, 2014, **48**, 4844–4851.
- 93 B.-Y. Song, S. Gwak, M. Jung, G. Nam and N. Y. Kim, *Rapid Commun. Mass Spectrom.*, 2018, **32**, 235–240.
- 94 D. Hunkeler, R. U. Meckenstock, B. Sherwood Lollar, T. C. Schmidt, J. T. Wilson, T. Schmidt and J. Wilson, A



- Guide for Assessing Biodegradation and Source Identification of Organic Ground Water Contaminants Using Compound Specific Isotope Analysis (CSIA)*, US EPA, Washington, D.C., 2008.
- 95 E. Passeport, N. Zhang, L. Wu, H. Herrmann, B. Sherwood Lollar and H. H. Richnow, *Water Res.*, 2018, **135**, 95–103.
- 96 M. Marchesi, L. Alberti, O. Shouakar-Stash, I. Pietrini, F. de Ferra, G. Carpani, R. Aravena, A. Franzetti and T. Stella, *Sci. Total Environ.*, 2018, **619–620**, 784–793.
- 97 L. Fishbein, Anthropogenic Compounds, in *The Handbook of Environmental Chemistry*, Springer, Berlin, Heidelberg, 1984, vol. 3/3C, pp. 1–40.
- 98 A. C. Borba da Cunha, M. J. López de Alda, D. Barceló, T. M. Pizzolato and J. H. Z. dos Santos, *Anal. Bioanal. Chem.*, 2004, **378**, 940–954.
- 99 M. Skarpeli-Liati, A. Turgeon, A. N. Garr, W. A. Arnold, C. J. Cramer and T. B. Hofstetter, *Anal. Chem.*, 2011, **83**, 1641–1648.
- 100 S. Reinnicke, A. Bernstein and M. Elsner, *Anal. Chem.*, 2010, **82**, 2013–2019.
- 101 H. K. V. Schürner, M. P. Maier, D. Eckert, R. Brejcha, C.-C. Neumann, C. Stumpp, O. A. Cirpka and M. Elsner, *Environ. Sci. Technol.*, 2016, **50**, 5729–5739.
- 102 L. Carena, D. Fabbri, M. Passananti, M. Minella, M. Pazzi and D. Vione, *Chemosphere*, 2020, **246**, 125705.
- 103 T. Katagi, *J. Pestic. Sci.*, 2018, **43**, 57–72.
- 104 C. M. Aelion, P. Höhener, D. Hunkeler and R. Aravena, *Environmental Isotopes in Biodegradation and Bioremediation*, CRC Press, Boca Raton, 2009.
- 105 M. Skarpeli-Liati, M. Jiskra, A. Turgeon, A. N. Garr, W. A. Arnold, C. J. Cramer, R. P. Schwarzenbach and T. B. Hofstetter, *Environ. Sci. Technol.*, 2011, **45**, 5596–5604.
- 106 S. Hussain, M. Arshad, D. Springael, S. R. S. Rensen, G. D. Bending, M. Devers-Lamrani, Z. Maqbool and F. Martin-Laurent, *Crit. Rev. Environ. Sci. Technol.*, 2015, **45**, 1947–1998.
- 107 H. Boucheloukh, W. Remache, F. Parrino, T. Sehili and H. Mechakra, *Photochem. Photobiol. Sci.*, 2017, **16**, 759–765.
- 108 M. Canle López, M. I. Fernandez, S. Rodríguez, J. A. Santaballa, S. Steenken and E. Vulliet, *ChemPhysChem*, 2005, **6**, 2064–2074.
- 109 F. Eissa, N. E.-H. Zidan and H. Sakugawa, *Geochem. J.*, 2015, **49**, 309–318.
- 110 F. Ruggieri, A. A. D'Archivio, M. Fanelli and S. Santucci, *RSC Adv.*, 2011, **1**, 611–618.
- 111 S. Kanan, M. A. Moyet, R. B. Arthur and H. H. Patterson, *Catal. Rev.*, 2020, **62**, 1–65.
- 112 S. Nélieu, F. Perreau, F. Bonnemoy, M. Ollitrault, D. Azam, L. Lagadic, J. Bohatier and J. Einhorn, *Environ. Sci. Technol.*, 2009, **43**, 3148–3154.
- 113 K. Kovács, J. Farkas, G. Veréb, E. Arany, G. Simon, K. Schrantz, A. Dombi, K. Hernádi and T. Alapi, *J. Environ. Sci. Health, Part B*, 2016, **51**, 205–214.
- 114 M. E. A. Kribéche, H. Mechakra, T. Sehili and S. Brosillon, *Environ. Technol.*, 2016, **37**, 172–182.
- 115 D. Sarr, C. Diop, L. Cisse, O. H. m. Isselmou, M. Mbaye, F. Delattre, O. Oyelakin, M. D. G. Seye, A. Coly and A. Tine, *J. Chem.*, 2014, **2**, 85–103.
- 116 B. Jin and M. Rolle, *Environ. Pollut.*, 2016, **210**, 94–103.
- 117 M. Siampiringue, R. Chahboune, P. Wong-Wah-Chung and M. Sarakha, *Soil Syst.*, 2019, **3(1)**, 17.
- 118 Y. Liu, F.-B. Li, W. Xia, J.-M. Xu and X.-S. Yu, *Chemosphere*, 2013, **91**, 1547–1555.
- 119 C. Aeppli, M. Tysklind, H. Holmstrand and O. Gustafsson, *Environ. Sci. Technol.*, 2013, **47**, 790–797.
- 120 Y. Xu, Y. He, Q. Zhang, J. Xu and D. Crowley, *Environ. Sci. Technol.*, 2015, **49**, 5425–5433.
- 121 M. M. Broholm, D. Hunkeler, N. Tuxen, S. Jeannotat and C. Scheutz, *Chemosphere*, 2014, **108**, 265–273.
- 122 M. Rosell, J. Palau, S. H. Mortan, G. Caminal, A. Soler, O. Shouakar-Stash and E. Marco-Urrea, *Sci. Total Environ.*, 2019, **648**, 422–429.
- 123 G. P. Lahm, J. Desaegeer, B. K. Smith, T. F. Pahutski, M. A. Rivera, T. Meloro, R. Kucharczyk, R. M. Lett, A. Daly, B. T. Smith, D. Cordova, T. Thoden and J. A. Wiles, *Bioorg. Med. Chem. Lett.*, 2017, **27**, 1572–1575.
- 124 H. Lin, K. Pang, Y. Ma and J. Hu, *Chemosphere*, 2018, **214**, 543–552.
- 125 L. Wu, S. Moses, Y. Liu, J. Renpenning and H. H. Richnow, *Anal. Chim. Acta*, 2019, **1064**, 56–64.
- 126 H. Ma, L. Pan, A. Li and Z. Zhang, *Chin. J. Pestic. Sci.*, 2017, **19**, 282–289.
- 127 P. Alvarez-Zaldivar, S. Payraudeau, F. Meite, J. Masbou and G. Imfeld, *Water Res.*, 2018, **139**, 198–207.
- 128 L. M. Canle, M. I. Fernández and J. A. Santaballa, *J. Phys. Org. Chem.*, 2005, **18**, 148–155.
- 129 V. Ponsin, C. Torrento, C. Lihl, M. Elsner and D. Hunkeler, *Anal. Chem.*, 2019, **91**, 14290–14298.
- 130 D. P. Hessler, V. Gorenflo and F. H. Frimmel, *Acta Hydrochim. Hydrobiol.*, 1993, **21**, 209–214.
- 131 A. H. Meyer and M. Elsner, *Environ. Sci. Technol.*, 2013, **47**, 6884–6891.
- 132 C. Lihl, B. Heckel, A. Grzybkowska, A. Dybala-Defratyka, V. Ponsin, C. Torrento, D. Hunkeler and M. Elsner, *Environ. Sci.: Processes Impacts*, 2020, **22**, 792–801.
- 133 C. Lihl, J. Renpenning, S. Kummel, F. Gelman, H. K. V. Schurner, M. Daubmeier, B. Heckel, A. Melsbach, A. Bernstein, O. Shouakar-Stash, M. Gehre and M. Elsner, *Anal. Chem.*, 2019, **91**, 12290–12297.
- 134 I. Yankelzon, T. Engelman, A. Bernstein, H. Siebner, Z. Ronen and F. Gelman, *Environ. Sci. Pollut. Res. Int.*, 2020, **27**, 22749–22757.
- 135 H. Liang, N. Bilon and M. T. Hay, *Water Environ. Res.*, 2014, **86**, 2132–2155.
- 136 T. Miyawaki, M. Sugihara, S. Hirakawa, T. Hori, J. Kajiwara, S. Katsuki, C. Mitoma and M. Furue, *Environ. Sci. Pollut. Res. Int.*, 2018, **25**, 16464–16471.
- 137 D. Zhang, S.-Z. Cao, X.-L. Duan and J. Yao, *China Environ. Sci.*, 2018, **38**, 2714–2721.
- 138 C. Griebler, L. Adrian, R. U. Meckenstock and H. H. Richnow, *FEMS Microbiol. Ecol.*, 2004, **48**, 313–321.



- 139 C. Torrentó, R. Bakkour, G. Glauser, A. Melsbach, V. Ponsin, T. B. Hofstetter, M. Elsner and D. Hunkeler, *Analyst*, 2019, **144**, 2898–2908.
- 140 A. Bernstein, O. Shouakar-Stash, K. Ebert, C. Laskov, D. Hunkeler, S. Jeannotat, K. Sakaguchi-Söder, J. Laaks, M. A. Jochmann, S. Cretnik, J. Jager, S. B. Haderlein, T. C. Schmidt, R. Aravena and M. Elsner, *Anal. Chem.*, 2011, **83**, 7624–7634.
- 141 J. Renpenning, A. Horst, M. Schmidt and M. Gehre, *J. Anal. At. Spectrom.*, 2018, **33**, 314–321.
- 142 P. Sivaperumal, A. Salauddin, A. R. Kumar, K. Santhosh and T. Rupal, *Food Anal. Methods*, 2017, **10**, 2346–2357.
- 143 P. Sandín-España, B. Sevilla-Morán, C. López-Goti, M. M. Mateo-Miranda and J. L. Alonso-Prados, *Arabian J. Chem.*, 2015, **9**, 694–703.
- 144 S. Christian, P. Pradhan and U. Jans, *J. Agric. Food Chem.*, 2018, **66**, 424–431.
- 145 B. Jiang, N. Jin, Y. Xing, Y. Su and D. Zhang, *Crit. Rev. Biotechnol.*, 2018, **38**, 1025–1048.
- 146 N. Fohrer, A. Dietrich, O. Kolychalow and U. Ulrich, *J. Environ. Qual.*, 2014, **43**, 75–85.
- 147 T. Tsuchiyama, M. Katsuhara and M. Nakajima, *J. Chromatogr. A*, 2017, **1524**, 233–245.
- 148 L. Yeasmin, S. A. Macdougall and B. D. Wagner, *J. Photochem. Photobiol., A*, 2009, **204**, 217–223.
- 149 M. P. Maier, S. Qiu and M. Elsner, *Anal. Bioanal. Chem.*, 2013, **405**, 2825–2831.
- 150 A. H. Meyer, H. Penning, H. Lowag and M. Elsner, *Environ. Sci. Technol.*, 2008, **42**, 7757–7763.
- 151 A. Cincinelli, F. Pieri, Y. Zhang, M. Seed and K. C. Jones, *Environ. Pollut.*, 2012, **169**, 112–127.
- 152 J. Renpenning, K. L. Hitzfeld, T. Gilevska, I. Nijenhuis, M. Gehre and H. H. Richnow, *Anal. Chem.*, 2015, **87**, 2832–2839.

